

Review

Self-Immobilizing Quinone Methides for the Fluorescent Sensing of Enzyme Activity

Dóra Kern^{1,2,*}  and Attila Kormos^{1,*} 

- ¹ Chemical Biology Research Group, Institute of Organic Chemistry, ELKH Research Centre for Natural Sciences, Magyar Tudósok Krt 2, 1117 Budapest, Hungary
- ² Hevesy György PhD School of Chemistry, Eötvös Loránd University, Pázmány Péter sétány 1/a., H-1117 Budapest, Hungary
- * Correspondence: kern.dora@ttk.hu (D.K.); kormos.attila@ttk.hu (A.K.)

Abstract: Gaining insight into biological processes relies on sensitive analytical techniques. These often require labeling of biomolecules that help visualize them. Selective covalent labeling without preliminary modification of the biomolecules is an advantageous method. For example, this can be achieved by using probes that are capable of in situ quinone methide (QM) formation. The QM can be masked to give a stable precursor, and the highly reactive form is only generated upon activation by a specific trigger. The in situ formed QM then binds covalently to the nucleophilic side chains of either the target protein or a protein in close proximity. Using fluorogenic probes further improves this method by reducing non-specific background signals, thus improving signal-to-noise ratios. In this review we summarize the development of quinone methide-based probes from mechanism-based inactivation to red-emitting, fluorogenic activity probes, focusing on enzyme-triggered activation.

Keywords: quinone methides; fluorescence; activity probes; fluorogenic probes; self-immobilization



Citation: Kern, D.; Kormos, A. Self-Immobilizing Quinone Methides for the Fluorescent Sensing of Enzyme Activity. *Chemosensors* **2023**, *11*, 155. <https://doi.org/10.3390/chemosensors11030155>

Academic Editors: Guo-Hui Pan, Hongshang Peng and Biao Dong

Received: 24 January 2023

Revised: 16 February 2023

Accepted: 21 February 2023

Published: 23 February 2023



Copyright: © 2023 by the authors. Licensee MDPI, Basel, Switzerland. This article is an open access article distributed under the terms and conditions of the Creative Commons Attribution (CC BY) license (<https://creativecommons.org/licenses/by/4.0/>).

1. Introduction

Targeted covalent modification of biomolecules using small molecules in biological media has gained ground in the last decades [1–5]. The most often used reactions between exogenous electrophiles and biological nucleophiles to label and/or alter the function of the target molecule are nucleophilic substitutions and Michael additions [6]. Owing to the variety of nucleophiles present in biological media, using reactive electrophiles can lead to non-specific reactions. One of the possibilities to avoid non-specific ligation with biomolecules is the masking of reactive functional groups. This blocked compound shows no reactivity towards either targets or off-target molecules until the reactive form is generated in situ by a trigger effect. One straightforward approach to accomplish controlled masking and targeted release is the application of quinone methides (QMs) [7].

QMs can be characterized as quinone analogues in which one of the carbonyl oxygens is replaced by a methylene group. Both 1,2-QMs (*ortho*-QMs) and 1,4-QMs (*para*-QMs) display significant electrophilic reactivity (Figure 1a) that can be explained with their zwitterionic aromatic valence bond resonance structure [8]. The rarely-encountered meta-derivative is also possible, however, it exhibits higher instability than its isomers [9]. The formation of azaquinone methides is also feasible if the oxygen of the quinone methide function is replaced by nitrogen (Figure 1a). Despite their high reactivity, the QMs can be blocked in the form of a stable precursor. In this precursor, the phenolic oxygen is substituted by a recognizable unit, while the methylene group of the QM is masked with an adequate leaving group. As a result of a trigger—in biological media mostly enzymatic activity, a biological analyte, or reactive oxygen species (ROS)—both the recognizable unit and the leaving group are cleaved from the molecule, generating the QM in situ (Figure 1b). The formed QM is rapidly attacked by a nucleophilic moiety, usually amino and thiol groups or water.

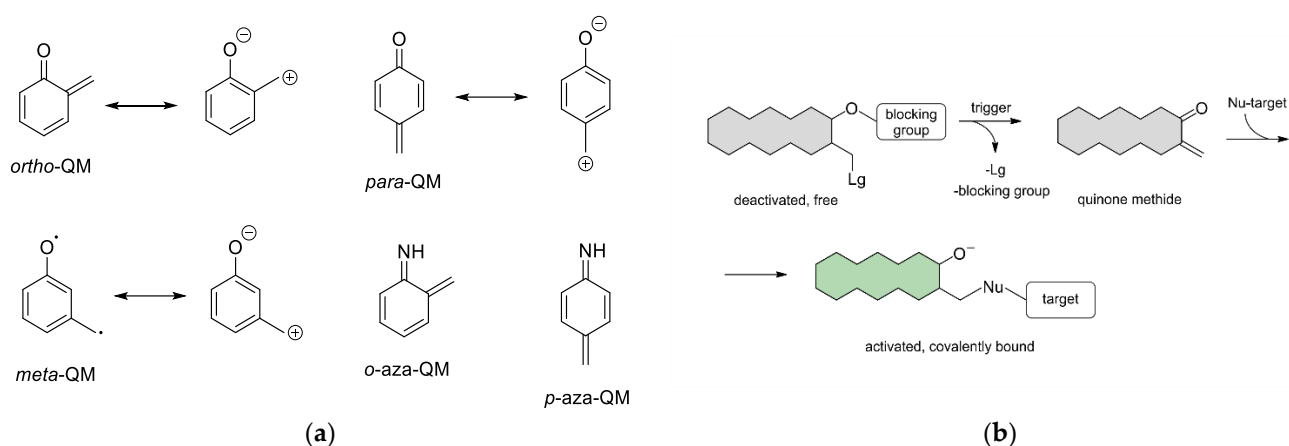


Figure 1. (a) Isomers of quinone methide and their zwitterionic resonance structure. *Ortho*- and *para*-aza-quinone methides. (b) Cartoon representation of QM generation.

The aim of this review is to demonstrate the versatility of compounds utilizing the quinone methide function. We focused on sensing and monitoring enzyme activity with mechanism-based enzyme inhibition and enzyme activity-based probes for many enzyme classes, including phosphatases, glycosidases, sulfatases, and β -lactamases, emphasizing the importance of selective fluorescent labeling. We first showed the early application of QMs for enzyme inhibition, then the utilization of fluorescent labeling and signaling of enzyme activity. The structure of the probes is highly modular, and we hope that this review will help researchers to choose the best combination of trigger, leaving group, and fluorophore that best suits their intended use. We also comment on the possible future applications of QMs in the conclusion to widen the scope of labeling enzymes and possibly other biomolecules of interest.

2. Enzyme Inhibition

The first published examples of achieving enzyme inhibition with QMs date back to the 1970s and 1980s, although these early implementations utilize chloride as a leaving group leading to the generation of QMs [10–12]. Although the application of the highly reactive benzylchlorides may run the risk of non-specific alkylation and inhibition of biomolecules, these results paved the way for the biological utilization of QMs.

In search of a selective enzyme activated inhibitor for glycosidases, Halazy and coworkers replaced the chloride leaving group with the more stable fluoride inspired by their previously reported acyl fluoride generating 1,1-difluoroalkyl glucosides [13]. The combination of QMs with the milder reactivity of fluorine-containing compounds led to the synthesis of *ortho*- and *para*-(difluoromethyl)aryl- β -glucosides providing the first target-selective enzyme inhibition utilizing QM chemistry (Figure 2) [14]. Upon β -glucosidase catalyzed hydrolysis, the molecule decomposes to glucose and the corresponding fluorinated phenol derivative. The latter compound loses hydrogen fluoride, and the reactive QM motif is obtained, attaching itself covalently to the nucleophilic active center (Figure 2). It was shown that the hydrolysis rate of *ortho*- and *para*-difluoromethyl substituted glucosides was comparable, and that the incorporation of electron withdrawing alkoxy groups to the molecule yielded slightly decreased cleavage reaction rates.

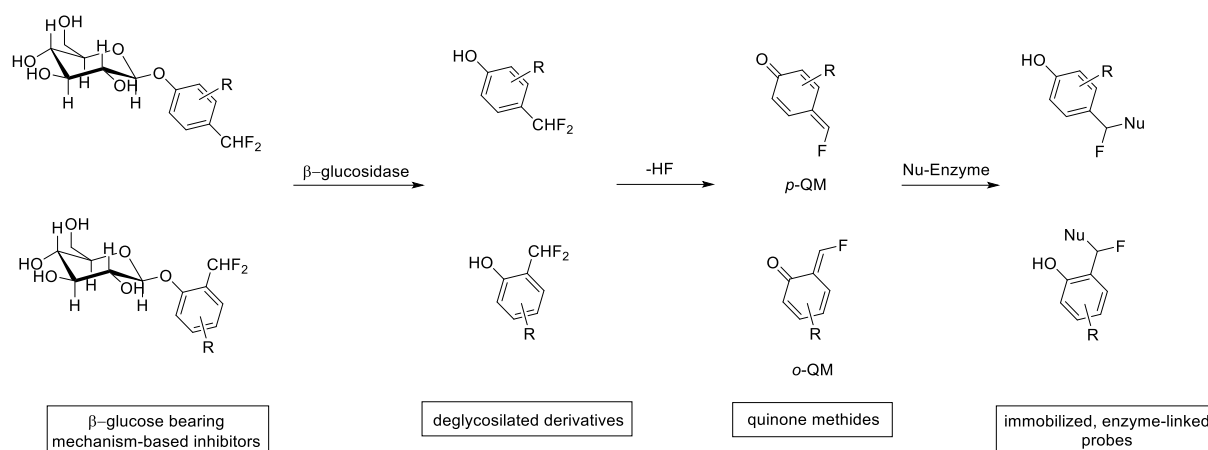


Figure 2. General structure of the *ortho*- and *para*-(difluoromethyl)aryl- β -glucosides, activation cascade upon β -glucosidase activity, and the subsequent ligation with a nucleophilic side chain of the enzyme of interest (“Nu-Enzyme”).

Wakselman and coworkers applied nitrobenzyl derivatives that, upon bioreduction, generated aza-QMs (“quinonimide methides”) [15]. Although their original goal was the liberation of carboxylic acids, they state that the formed aza-QMs can alkylate DNA or other biomolecules, contributing to the antitumor effect. A later work focused more on the direct effect of aza-QMs in trypsin-like serine protease inhibition [16]. Here, the latent aza-QM was incorporated to a functionalized cyclopeptide and was generated with the cleavage of bromide and sulfide leaving groups. Myers and Widlanski described the first phosphotyrosine phosphatase (PTPase) inhibitor of such kind [17], aiming for better understanding of tumor suppression by blocking human prostatic acid (PAP) with 4-(fluoromethyl)phenyl phosphate (FMPP). The effect of nucleophilic scavenging agents for inactivation was also examined, proving that the excess of neither cysteine, sodium azide, nor dithiothreitol affected the process negatively. The difluoro-analogue of this inhibitor, 4-(difluoromethyl)phenyl phosphate, was described by Wang and coworkers at the same time [18]. This difluorinated derivative is believed to be more stable in aqueous media, which is consistent with the slower $t_{1/2}$ measured for PAP inactivation. Although FMPP displayed good inactivation rates, its properties were far from ideal: inactivation was shown not only towards PAP enzyme [19], and it was also limited by its instability in water and buffers. To improve these factors, Myers and coworkers developed their inhibitor further by introducing a nitro-group to the 2-position [20]. The obtained 4-fluoromethyl-2-nitrophenyl phosphate, despite being the substrate of PAP, did not result in the inactivation of the enzyme due to the improved stability, but the modification allowed the change of the leaving group from fluoride to the more active chloride and bromide. The mechanism-based inhibition of glucosamine 6-phosphate synthase (GlmS) was also carried out for the first time with 1- γ -glutamyl-2-[(*p*-difluoromethyl)phenylthio]glycine to investigate the antibacterial and antifungal activity of its glutamine site-directed inhibitors [21]. Another thio-QM-based idea abolished the *enterococci* resistance to vancomycin, a glycopeptide antibiotic used in therapy [22,23], by inhibiting the activity of VanX protein, a D-alanyl-D-alanine dipeptidase. However, the achieved inactivation efficiency was low.

After designing several suicide inhibitors for enzymes, the focus was on expanding the application range of these inactivator properties. The selective trigger-induced, in situ-generated reactive species and the subsequent covalent ligation is an ideal basis for the construction of combinatorial chemical systems [24–28].

3. Activity-Based Probes

As it was shown, mechanism-based inactivators, also called as suicide inhibitors, are activated in situ as a result of the enzyme activity that is wished to be blocked. The generated reactive QM alkylates the active site of the enzyme, thus inactivating it. Activity probes

work on the same basis, but with a different aim: in this case, the covalent modification does not necessarily occur on the active site. The focus is on preserving spatial information, thus not letting the probe diffuse away from the proximity of the enzyme. This feature makes the activity probes suitable for highly specific labeling purposes without the need for protein modification. Up to now, several enzymes, such as phosphatases, glycosidases, hydrolases, and proteases, were studied this way.

3.1. Phosphatases

Protein phosphatases are responsible for protein dephosphorylation, that is, removing a phosphate group from a tyrosine, serine, or threonine residue. Lo and coworkers synthesized the first activity probe for protein tyrosine phosphatases (PTPases) which contained a coumarin unit as a fluorescent reporter [29]. Despite the novelty of the probe, no comprehensive study was carried out regarding selectivity or sensitivity.

Three years later the same authors paved the way further for activity-based probes, as they were the first to describe a class-selective probe for protein tyrosine phosphatases [30]. They prepared activity probes for protein tyrosine phosphatase 1B (PTP1B) that contained a phosphate monoester recognition head for PTP1B, a latent *p*-QM unit (“trapping device”), a linker, and a reporter group (Figure 3). This latter moiety was either dansyl (LCL-1), which enables fluorescent labeling of protein, or biotin, through which sensitive secondary-detection is possible (LCL-2). It was shown in SDS-PAGE-labeling experiments that both compounds were selective for phosphatases compared to trypsin and β -galactosidase. The authors carried out labeling experiments in the presence of other proteins, such as albumin or phosphorylase b, but detected no signal for these on the gels. The time needed for the fluoride elimination was also studied with ^{19}F NMR in the case of the dansyl-containing LCL-1, monitoring the peaks of inorganic fluoride and the starting material. The peak of the starting material disappeared in 96 h. During this, no enzyme inhibition was observed.

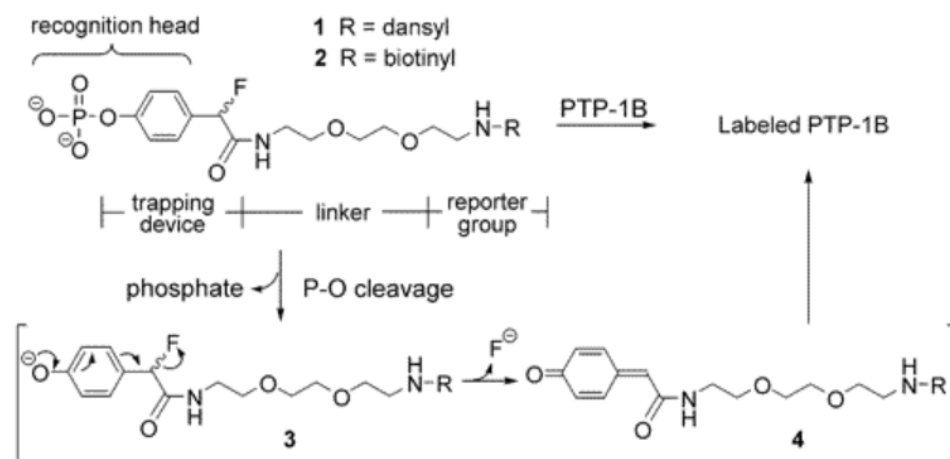


Figure 3. The structure of LCL-1 and LCL-2 and the mechanism of substrate cleavage. Reprinted with permission from [30], copyright 2002 American Chemical Society.

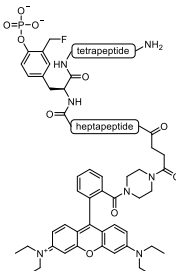
Using dyes with fluorescent emission towards higher wavelengths is advantageous as they avoid autofluorescence, thus improving the quality of labeling. Zhu and colleagues described activity-based probes that contain a Cy3 dye and target phosphatase activity [31]. Upon activation by the enzyme the two probes generate *o*- and *p*-QM, respectively, and both are capable of labeling PTPs and other phosphatases, such as alkaline phosphatases. Even though all phosphatases showed affinity towards the probes, members of other enzyme families (lipases, proteases) were not labelled.

Shen and coworkers developed this concept further by incorporating the latent QM to a peptide sequence [32,33]. They synthesized an unnatural amino acid residue of phosphotyrosine that contains a difluoromethyl group in the *ortho* position. This recognition unit was specified for PTP-1B and was linked with a PEG-chain to biotin as a reporter unit.

The probe displayed concentration-dependent selectivity: 200 μM caused biotin labeling of both PTP1B and another PTP recombinant, PTP4A3, while 20 μM was selective to PTP1B. When the enzyme was inherently blocked, the probe did not bind to the protein, indicating that enzyme activity is needed for the process. It was also shown that one protein was labeled on multiple nucleophilic side chains and labeling yielded the inactivated enzyme. The authors performed the labeling in lysates, and they concluded. both in *E. coli* and Jurkat cell lysates, that adding a competing PTP inhibitor to the system facilitates the PTP1B labeling without nonspecific labeling of other phosphatases.

The incorporation of latent QMs to unnatural amino acids was carried out by Kalesh and coworkers as well [34], who wished to enable target-specific binding to different PTPs. This selective recognition was assured by the peptide sequence to which the unnatural amino acid residue was incorporated. The labeling was carried out with a rhodamine attached to the C-terminus of the short peptide chain. The peptide sequences were designed in accordance with the substrate recognition of a given enzyme. Five PTPs (PTP1B, TCPTP, SHP1, SHP2, LMWPTP) were tested with ten activity probes, with the obtained response (i.e., the intensity of fluorescent emission) corresponding well with the substrate preference. Besides labeling, the probes displayed concentration- and time-dependent inactivation of the enzymes (Table 1). One of the selective PTP1B inhibitors was also tested in HEK293T and NIH3T3 cell lysates, with the latter having very low endogenous PTPB1 expression. As indicated by Western blotting, 10 μM of probe concentration could detect 5 ng PTP1B enzyme in the HEK293T lysate, which highlights the feasibility of the described method.

Table 1. Kinetic data of the enzyme inhibition of probes from [34].

Structure	Target Enzyme	k_i (min^{-1})	K_i (mM)	Selectivity between PTPs	
	GGDEGIHXSELI	SHP1	0.78	2.81	moderate selectivity
	GGGSAAPXLKTK	PTPB1/TCPTP	0.68	1.00	moderate selectivity
	GGKAVDGVKVPQ	PTP1B	0.71	0.97	high PTPB1 selectivity
	GGLNSDGYTPEP	LMWPTP	0.80	2.19	moderate selectivity
	GGLPPEGXVVVV	SHP2	0.74	3.89	moderate selectivity
	GGNSDVQXTEVQ	SHP1/SHP2	0.73	1.93	moderate selectivity
	GGPEGHEX _p YRVR	PTP1B	0.75	0.94	moderate selectivity
	GGPQDKEXYKVK	SHP2/PTP1B	0.75	2.45	moderate selectivity
	GGVDADEXLIPQ	SHP2/PTP1B	0.71	1.48	moderate selectivity
	GGELEFXMDE	PTP1B	0.61	1.00	moderate selectivity

Independently at the same time, Huang and coworkers aimed to carry out specific activity-based probes for different PTPs as well [35]. They also incorporated peptide segments as recognizable unit and three tripeptide-containing probes were synthesized: a leucinamide at the C-terminus, then the modified, latent QM-containing phosphotyrosine derivative, and either Glu, Phe, or Lys at the N-terminus. A biotin reporter was attached to the N-terminus through an ethylene glycol linker. Neither of the three probes showed activity towards non-phosphatase enzymes (carbonic anhydrase, γ -globulin, phosphorylase b, RNase A, and lysozyme) or non-PTP phosphatases (ALP, PTEN, PPP1CA, PPM1A). Five PTP enzymes were also studied (PTP1B, TCPTP, SHP2, VHR, PTP-PEST): one had no substrate preference, while four showed increased affinity towards a certain sequence, but no exclusive labeling could be achieved. Another drawback of the synthesized probes was the high instability in the absence of the target enzyme, which showed a 10% hydrolysis in aqueous media after 1 h.

Polaske and colleagues utilized QMs to label solid-phase proteins which can be used in immunoassays [36]. In this study, a primary antibody recognized an antigen attached to the surface, followed by the incubation of an alkaline phosphatase-secondary antibody conjugate (Figure 4). The activity-based QM precursor was applied via the hydrolysis of substrate and subsequent QM generation bound to a nucleophile in close proximity, either

to the antibody complex or water. The probe was visualized either with DAB-detection or fluorescent microscopy, depending on the attached reporter group being biotin or Cy5-dye, respectively. As for the leaving group, difluoromethyl and monofluoromethyl groups were utilized. The effect of pH was studied first by the difluoromethyl derivative: at pH 7.0 no specific fluorescent signal was detected, meaning the fluorescent signal was spread all over the FFPE tonsil tissue. An alkaline pH would deprotonate the phenol and increase the rate of QM formation, and increasing the pH yielded slightly less background fluorescence, but not even pH 11 could exclude nonspecific labeling. To get specifically bound dyes, the authors wanted to accelerate the rate of fluoride elimination and QM formation as well as reaction with a nucleophile. They hypothesized that monofluoromethyl group as the leaving group would result in a more labile QM, and therefore decided to utilize this. At pH 8.5, the monofluoromethylated probe showed diminished overall diffusion, and at pH 7.0–8.0 high diffusion could still be observed. Monofluorinated Cy5 probe was also synthesized, and the immunoassay at pH 10.0 yielded better signal-to-noise ratios at 1–5 μM .

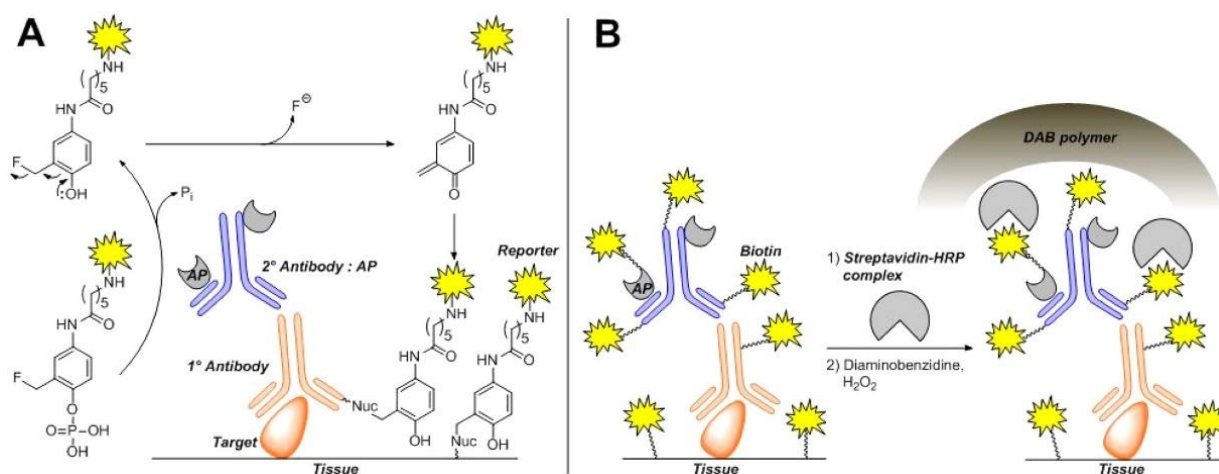


Figure 4. (A) Mechanism of covalent ligation to the target protein complex and (B) visualization of biotinylated probes with 3,3'-diaminobenzidine (DAB). Reprinted with permission from [36], copyright 2016 American Chemical Society.

The labeling efficiency of different self-immobilizing probes were also studied with an alkaline phosphatase substrate system [37]. Ten activity-based probes were synthesized (Figure 5) with both latent *o*- and *p*-QM moieties, three linkers; difluoromethyl, fluoromethyl or ethyl carbamate leaving groups and either fluorescein or the NIR emitting P-Mero4 dye. All fluorescein-containing probes were tested in PBS buffer, and after 1 h, incubation with ALP enzyme SDS-PAGE was carried out (Figure 5). The fluorescent signal was stronger in the case of *p*-QMs than *o*-QMs, indicating a more efficient labeling (ALP-3, ALP-4, ALP-5), and not even a *o*- and *p*-QM-containing probe (ALP-6) showed stronger fluorescence. However, the probes, especially ALP-3, showed nonspecific labeling of BSA, even in the absence of the activating ALP, implying the instability of the probe. Changes in the structure led to decreased off-target labeling: the replacement of fluoride led to a less reactive ethyl carbamate leaving group and the linker L-III to L-I (ALP-6). The affinity of ALP-6 towards acid phosphatase (ACP) was also studied, but no labeling was seen, probably due to the acidic condition that did not favor QM formation. Live cell imaging was performed on ALP overexpressing HeLa cells and ALP-deficient HEK293T cells. In the former cell culture ALP-6 performed the best, while in the latter no signal could be detected. A detailed labeling mechanism was also proposed for ALP-5 and ALP-6. In the probes containing a P-Mero4 NIR dye (ALP NIR-1 and ALP NIR-2), 660 nm emission was observed both on BSA and ALP on gel. Live animal imaging yielded covalent ligation of probes to the enzyme, and the fluorescent signal was detectable after 24 h.

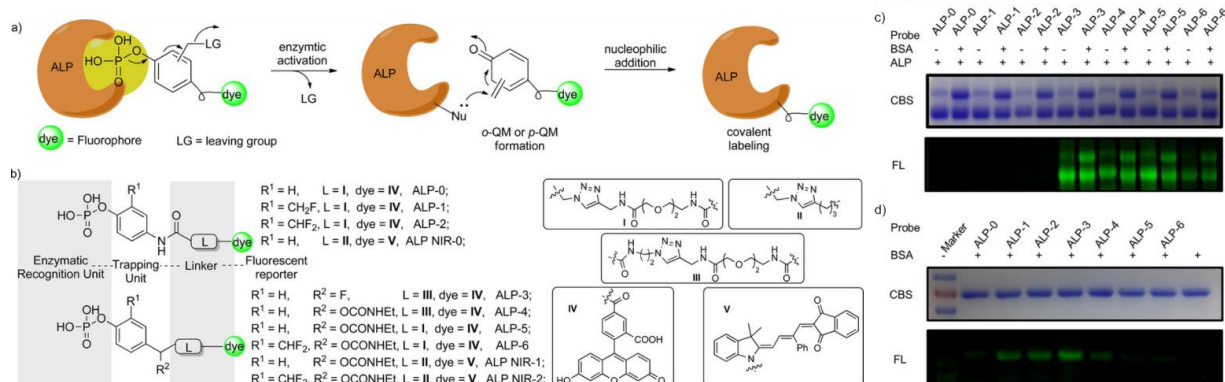


Figure 5. (a) Ligation mechanism of alkaline phosphatase activity-based probes and (b) the structure of the synthesized ALP and ALP-NIR probes. (c) Coomassie blue staining (CBS) and fluorescent (FL) imaging of ALP (12.5 U mL⁻¹) enzyme with the activity probes (7.5 μM, 1 h incubation) in the presence or absence of BSA (0.15 mg mL⁻¹) at 37 °C. (d) Imaging of BSA with the probes (7.5 μM, 1 h incubation) in the absence of ALP enzyme at 37 °C. Reproduced with permission from [37], copyright 2019 John Wiley and Sons.

For a summary of non-fluorogenic phosphatase probes, see Table 2.

The hitherto applied dyes do not ensure diminished background fluorescence, and the excess probes must be washed out from the sample. Fluorogenic behavior, caused by structural changes in the dye core accompanied with QM formation, could greatly improve the signal-to-noise ratio by decreasing background. However, up to this point, the built-in probe is usually quite distant from the aryl group of the latent QM unit and the covalent ligation site. In addition, utilizing fluorogenic turn-on dyes that do not dissociate from the site of activation would enable more precise monitoring of endogenous enzyme activity, thus using real-time cell imaging and FACS experiments. The fluorescence of push–pull dyes having a phenolate as the donor moiety can be quenched by substituting this phenolic oxygen. The removal of the substituent results in restored fluorescence [38]. Incorporating the enzyme substrate as the substituent of the phenolic OH results in fluorescence quenching and placing either a fluoromethyl or difluoromethyl group in the *ortho* position ensures the introduction of the latent QM. This way, the QM can be generated on the dye core as a result of enzyme-induced cleavage, and the subsequent dye–enzyme ligation provides non-diffusible labeling. Such fluorogenic systems are usually referred to as self-immobilizing probes.

The first fluorogenic PTP activity-based self-immobilizing probe was created by Ge and coworkers [39]. They based their work on the already-existing fluorogenic substrate of PTP, 6,8-difluoro-4-methylumbelliferone phosphate, but as this probe diffuses away from the activation site, further development was needed. An umbelliferone-containing unnatural amino acid was synthesized that not only was fluorogenic but could also be tailored to the desired PTP enzyme with elongation of peptide chains on the C- and N-termini. The probe contained a photolabile 2-nitrobenzyl group on the phosphate motif to facilitate chemical synthesis and provide temporal control for PTP-recognition. The authors incorporated the obtained pTyr mimicking amino acid to cell-penetrating peptides and studied one representative example (pER) and the probe as well. The UV light-induced uncaging of nitrobenzyl group was followed by fluorescence increment in the presence of PTP1B. However, the majority of this detected emission came from the water-quenched umbelliferone molecule, and only 10% of the probe was attached covalently to the enzyme, which did not solve the problem of diffusion. HeLa cells were incubated with the cell-penetrating peptides, but the same ligation rate was observed. Moreover, the needed UV-irradiation is not favorable for cells, so further improvement of this concept was needed.

Table 2. Non-fluorogenic activity-based probes for different phosphatases.

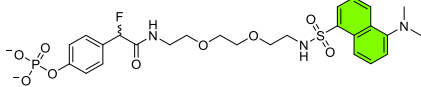
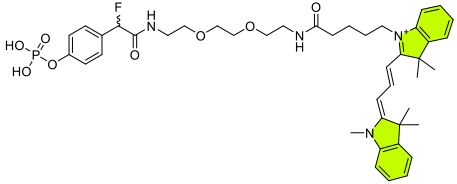
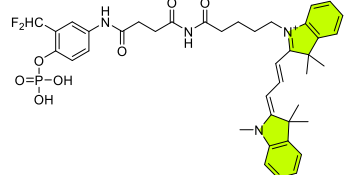
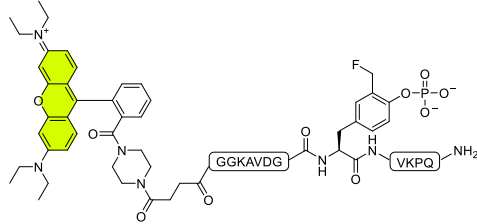
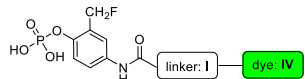
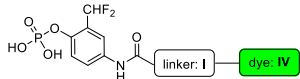
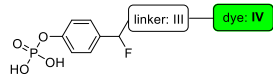
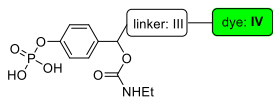
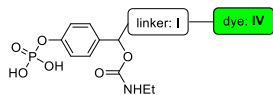
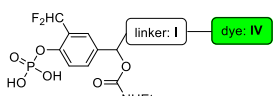
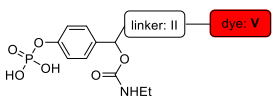
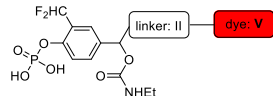
Structure ^a	Target Enzyme	λ (nm) abs/em ^b	Notes	Studied System	Ref.
	PTP1B	330/520	no cross-labeling in a mixture of proteins	in vitro	[30]
	PTP (yeast), ALPs (calf, shrimp, human)	555/565	selective against other enzyme classes, no selectivity among phosphatases	in vitro	[31]
	PTP (yeast), ALPs (calf, shrimp, human)	555/565	selective against other enzyme classes, no selectivity among phosphatases	in vitro	[31]
	PTP1B	540/565	high PTPB1 selectivity against other PTPs, no cross-labeling in cell lysates	in vitro	[34]
	ALP	490/520	low labeling efficiency	in vitro	[37] ^c

Table 2. Cont.

Structure ^a	Target Enzyme	λ (nm) abs/em ^b	Notes	Studied System	Ref. ^c
	ALP	490/520	low labeling efficiency	in cellulo (HeLa)	[37] ^c
	ALP	490/520	cross-labeling with other protein	in vitro	[37] ^c
	ALP	490/520	cross-labeling with other protein	in vitro	[37] ^c
	ALP	490/520	cross-labeling with other protein, most efficient labeling ^d in vitro	in cellulo (HeLa)	[37] ^c
	ALP	490/520	cross-labeling with other protein, most efficient labeling ^d in cellulo	in cellulo (HeLa)	[37] ^c
	ALP	620/670	cross-labeling with other protein, most efficient labeling ^e in vitro	in cellulo (HeLa), in vivo (mice)	[37] ^c
	ALP	620/670	cross-labeling with other protein, most efficient labeling ^e in cellulo, low cytotoxicity	in cellulo (HeLa), in vivo (mice)	[37] ^c

^a fluorophores are colored according to the approximate emission maxima. ^b approximate absorption and emission maxima. ^c for details of the structures, see Figure 5. ^d compared to the other fluorescein-containing ALP probes from [32]. ^e compared to the other NIR ALP probe from [32].

Li and coworkers designed a NIR-emitting, self-immobilizing fluorogenic probe that could be activated by ALP activity [40]. They introduced a phosphate group for the caging of fluorescence and a monofluoromethyl group to the applied NIR dye (Figure 6). However, the synthesized probe ALPIN-2 underwent rapid hydrolysis in PBS buffer (pH = 7.4) at 25 °C to ALPIN-OH. The change of the leaving group to ethyl carbamate resulted in elevated stability (ALPIN-3), probably due to the steric hindrance of ethyl carbamate, as ALP could not hydrolyze its substrate in comparison with the leaving group free molecule. This problem could be addressed by incorporating a spacer between the dye and the ALP recognition unit (ALPIN-5). This probe showed intensive fluorescent bands on SDS-PAGE with ALP and was also capable of labeling BSA in the presence of ALP. In live cell imaging, strong NIR fluorescence was observed in HeLa cells using ALPIN-5, even with no-wash conditions. ALPIN-5 was injected into living mice, and the fluorescent signal was detectable even after 48 h (Figure 6).

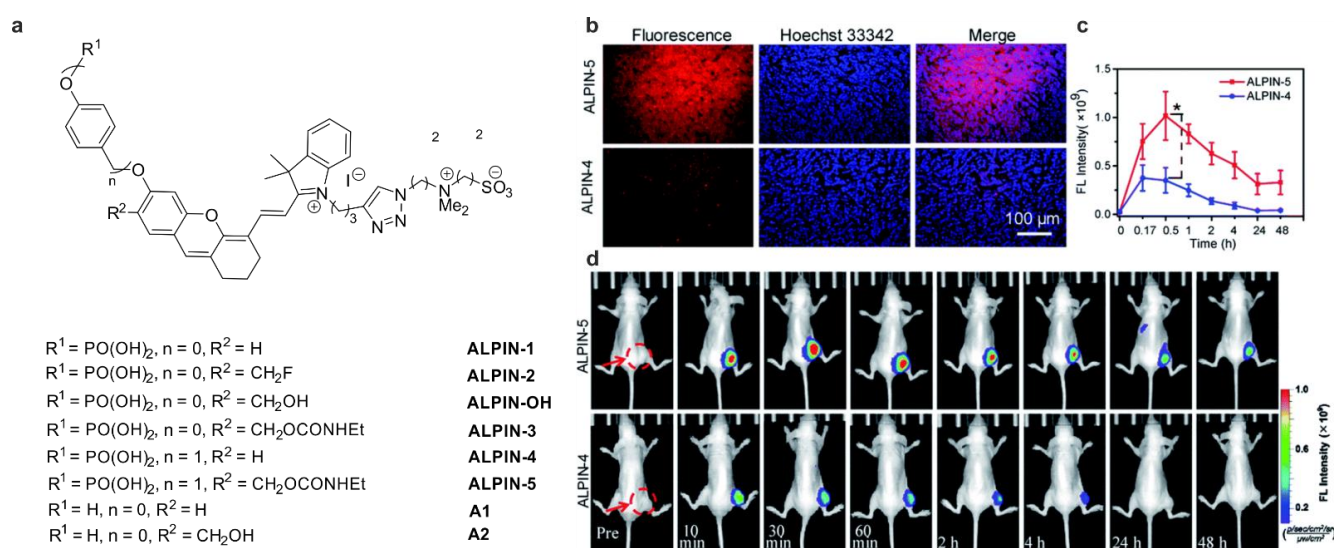


Figure 6. (a) Exact structures of the synthesized ALPIN dyes. (b) Fluorescent imaging of a tissue slice of a xenografted HeLa tumor in mice with immobilizing ALPIN-5 and non-immobilizing ALPIN-4 probes. (c) Fluorescent intensity of ALPIN-4 and ALPIN-5 after 48 h. (d) Imaging of ALP activity in mice in a 48 h time frame. Values are the mean \pm SD (* $p < 0.05$, $n = 3$). The red arrows and circles indicate the tumor locations in the mice. Adapted from [40], used under CC BY-NC 3.0.

The same group applied malachite green-based probes to monitor ALP activity [41]. Fluorogenicity was ensured by the very low fluorescent quantum yield exhibited by malachite green in aqueous environments because of its high conformational flexibility. The authors envisioned that binding to membrane proteins such as ALP would conformationally restrict the dye, thus enhancing the NIR fluorescence (670 nm). Malachite green was synthesized with three latent *p*-QM-containing units, caged with ALP substrates. In vitro study in PBS showed a 10-fold fluorescence increment upon ALP incubation and was attached to either ALP or the added nucleophile β -mercaptoethanol. No-wash, real-time imaging of live HeLa cells showed selective labeling of the cell membrane with no fluorescence inside the cell or photolability of the probe. As a result of cell imaging, the fluorescent turn-on ratio exceeded the in vitro measured data: the fluorescence was more than 100-fold stronger than in the absence of the probe.

For a summary of fluorogenic phosphatase probes, see Table 3.

Table 3. Fluorogenic activity-based probes for different phosphatases.

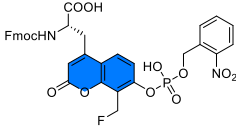
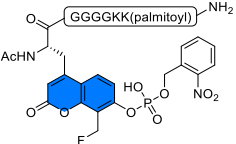
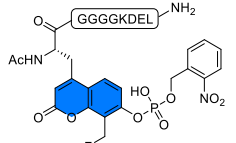
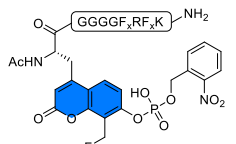
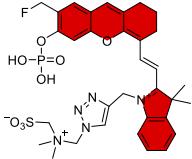
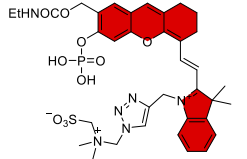
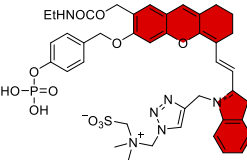
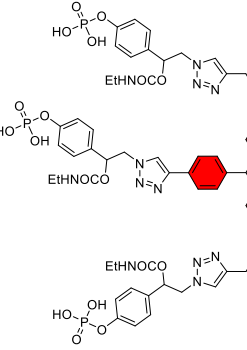
Structure ^a	Target Enzyme	Turn-On Ratio	λ (nm) abs/em ^b	Notes	Studied System	Ref.
	PTP	ND	360/460	in vitro model compound for the other probes in [34], low efficiency but specific labeling, no loss of enzyme activity, $k_{cat} = 8.8 \text{ s}^{-1}$, $K_M = 1.1 \text{ mM}$	in vitro	[39]
	PTP	ND	360/460	needs UV irradiation to uncage the active probe; localizes in plasma membrane	in cellulo (HeLa)	[39]
	PTP	ND	360/460	needs UV irradiation to uncage the active probe; localizes in ER	in cellulo (HeLa)	[39]
	PTP	ND	360/460	needs UV irradiation to uncage the active probe; localizes in mitochondria	in cellulo (HeLa)	[39]
	ALP	ND	685/720	unstable, hydrolyzes in PBS pH 7.4	in vitro	[40]

Table 3. Cont.

Structure ^a	Target Enzyme	Turn-On Ratio	λ (nm) abs/em ^b	Notes	Studied System	Ref.
	ALP	ND	685/720	stable, but ALP cannot hydrolyze the phosphate moiety	in vitro	[40]
	ALP	40 \times	685/720	cross-labeling with other protein, but in cellulo most of the fluorescence is detected in the plasma membrane, where ALP is located, low cytotoxicity	in cellulo (HeLa) in vivo (mice)	[40]
	ALP	10 \times ^c up to 200 \times ^d	633/655–685	higher photostability compared to the NIR dye from [32]; no cross-labeling studies, but in cellulo most of the fluorescence is detected in the plasma membrane, where ALP is located, low cytotoxicity	in cellulo (HeLa, HepG2, HCT116 cells)	[41]

^a fluorophores are colored according to the approximate emission maxima of the emissive form of the dye. ^b approximate absorption and emission maxima. ^c determined in vitro. ^d determined in cellulo.

3.2. Glycoside Hydrolases

Glycosidases play an important role in carbohydrate metabolism through hydrolyzing glycoconjugates into sugar units and aglycons. The first protocol utilizing QM chemistry for isolating glycosidases, namely *O*-linked *N*-acetylglucosaminidase, was described by Ichikawa and Ichikawa [42]. They synthesized biotinylated, *N*-acetylglucosamide substrate-containing probes that had different linkers and either a difluoromethyl or monofluoromethyl group in *ortho* position to the substrate (Figure 7). The probe was tested in buffer solution with the purified *N*-acetylglucosaminidase, and after 2 h of incubation at 37 °C the solution was treated with streptavidin-containing beads. The subsequent SDS-PAGE and visualization showed that difluoromethylated probe A was not efficient enough in labeling the enzyme, probably due to reasons attributed to the second fluorine atom (Figure 7). The disulfide bridge in B and C enabled a sulfide-exchange reaction between the probe and a cysteine residue in close proximity. This conjugate, however, could not be visualized due to the small amount of probe attached to the protein surface. To overcome non-efficient labeling displayed by A, a monofluoromethyl derivative was also synthesized (D) which showed attachment to the enzyme.

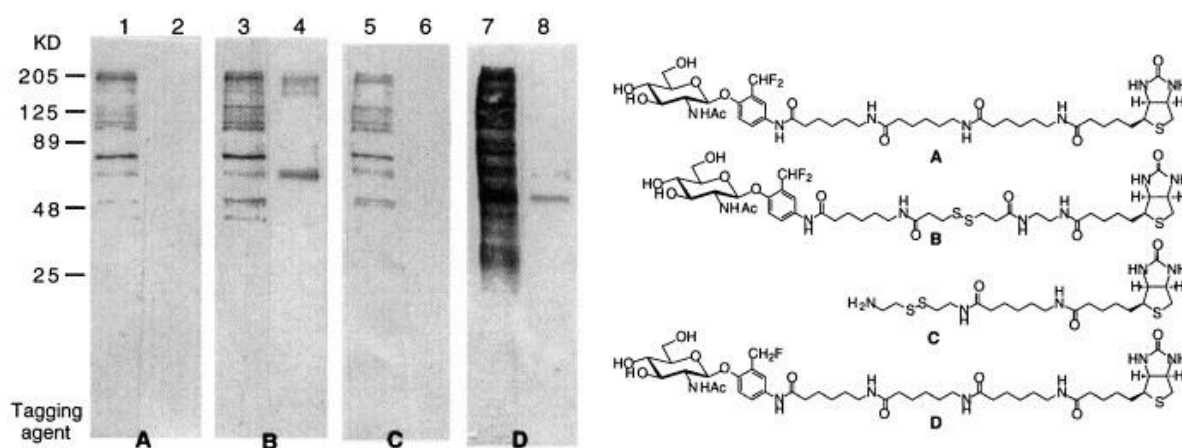


Figure 7. SDS-PAGE visualization of probes A–D before (lines 1, 3, 5, and 7) and after (2, 4, 6, and 8) affinity purification with streptavidin-agarose beads (left) and structure of the synthesized activity probes A–D. Reproduced with permission from [42], copyright 2001 Elsevier.

Analogously, an activity probe for β -glucosidase, was reported by Tsai and coworkers [43]. A β -glucose was attached to a *p*-hydroxybenzylic fluoride unit that is linked to a biotin. Both enantiomers of the probe were incubated with β -glucosidase and the reaction was followed with ^{19}F NMR. No difference occurred in the affinity towards the enzyme between the isomers. Gel electrophoresis was performed, indicating that multiple probes could have been attached to the enzyme. With high enzyme concentration (6.6 μM), no residual enzyme activity could be observed, which could be attributed either to aggregation of proteins or activity loss.

The first fluorescent, activity-based probe for glycoside hydrolases was designed by Kuroguchi et al. [44], utilizing a dansyl dye and an *o*-difluoromethyl moiety. The probe acted as a suicide substrate of five different β -galactosidases, and a fluorescent emission at 520 nm could be detected for all proteins. After the labeling, proteases were added to each enzyme to induce fragmentation and, with the application of antidansyl antibody and MALDI-TOF, labeled peptide fragments could be identified. This method was proven to be feasible in the recognition of catalytic domains as well. Live cell imaging indicated that inhibition could be prompted in murine B16 cancer cells.

It was shown earlier that QM chemistry is a useful tool in creating antibody libraries exhibiting β -galactosidase catalytic activity [24]. To widen the scope of antibodies capable of hydrolyzing different sugars, Shie and coworkers developed this concept further [45]. They

utilized the same recognition head-trapping device–linker–reporter group arrangement and tuned the recognition head to six sugars and anomeric configurations (α -D-Glc and β -D-Glc, α -D-Gal and β -D-Gal, α -L-Fuc and α -D-Man). By parallel syntheses, the glycosyl moiety could be easily replaced. Even though a detailed synthetic method was described, no application of the probes was demonstrated. A similar probe was described to monitor β -xylosidase activity [46].

β -galactosidase activity monitoring was carried out by combining QM chemistry and FRET (Figure 8) [47]. The reported probe consists of a 7-hydroxycoumarin as the energy donor and fluorescein as an energy acceptor, that is, exciting the coumarin at 400 nm, the emission of the fluorescein at 515 nm can be observed with a 93% FRET efficiency. Upon β -galactosidase catalytic activity (obtained from *E. coli*, encoded by *LacZ* gene), the carbamate leaving group is detached and the dissociated fluorescein diffuses away from the activation site. The QM is attacked by nucleophilic side chains of the protein, leading to covalent ligation accompanied by a distinct change in emission wavelength (460 nm instead of 515 nm), as no FRET occurs in the absence of fluorescein. This way, real-time monitoring of the reaction is easy and accurate. The labeled enzyme was also visualized with SDS-PAGE and ratiometric fluorescent microscopy of *LacZ*-positive HEK293 cells.

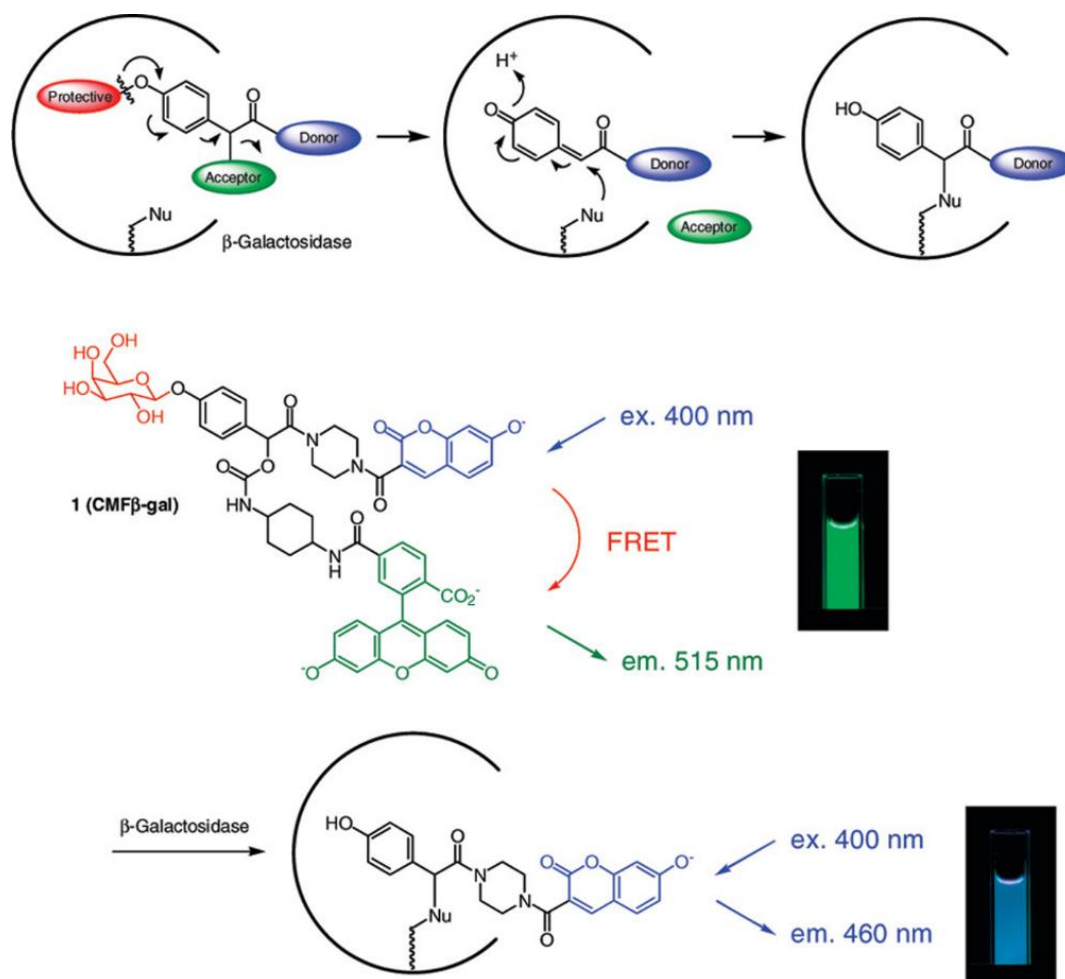


Figure 8. FRET-based β -galactosidase activatable probe CMF β -gal. Reprinted with permission from [47], copyright 2006 American Chemical Society.

Quenching of fluorescent probes is also possible with the introduction of a FRET-based quencher moiety. Kalidasan et al. utilized this concept when designing an α -N-acetylgalactosamine-containing quenched activity probe targeting α -N-acetylgalactosaminidase [48]. A dabcyl quencher unit ensures diminished fluorescence of the incorporated fluorescein dye. As a result of enzyme

activity, the dabcyyl moiety is liberated, leading to restored emission of the fluorescein at 520 nm. The probe was applied in the directed evolution of galactosidases with enhanced activity, as cells containing enzymes with different activities could be differentiated by their emission intensity after incubation with the probe.

Kwan and coworkers reported the synthesis of coumarin glycosides aiming for better resolution [49]. In this case, the generation of QM and the subsequent reaction is slow enough for the probe to dissociate from the active site, thus it will not behave as an inactivator of the enzyme. That is, choosing a difluoromethyl moiety would facilitate this due to its greater stability and longer reaction times compared to the monofluoromethyl-containing probes. Three methylumbelliferone-based activity probes were synthesized with a recognition unit specific to either D-glucuronic acid, D-glucose, or D-galactose. The authors first studied the expression of β -glucuronidase expression in plant cells with D-glucurono-probe, and as a result, the specific fluorescence of the coumarin could be detected in the stomata without background fluorescence and photobleaching of the dye. D-glucuro- and D-galacto-probes were employed in *E. coli* and yeast cells to which *Agrobacterium* sp. β -glucosidase/galactosidase was encoded. Covalent ligation proved to be successful as, after multiple washing cycles, the fluorescence of the probes did not diminish. This property enabled cell enrichment by FACS as well.

NIR glucuronide probes opened the door for in vivo imaging of β -glucuronidase activity [50]. Two analogous probes were designed, NIR-TrapG and FITC-TrapG, containing IR-820 and fluorescein isothiocyanate (FITC) dyes, respectively. The glucuronide recognition unit was attached to an *o*-difluoromethylphenol trapping unit. Preliminary experiments that were carried out with incubation of FITC-TrapG to either *E. coli* β -glucuronidase, mouse β -glucuronidase, or BSA showed that the probe displayed specific emission. More significantly, no enzyme inactivation was observed during the labeling, and the probe could attack either the target enzyme outside the active site or other bystander proteins. In vivo imaging was demonstrated on mice bearing subcutaneous CT26/m β G tumors. The measured fluorescence compared to the control CT26 cells were 4.59, 3.86, and 2.86 times stronger in the case of FITC-TrapG (525 nm) and 4.25, 4.92, and 5.21 times stronger in the case of NIR-TrapG (835 nm) after 24, 48, and 72 h, injected with 500 μ g/mouse and 100 μ g/mouse, respectively. Deep tissue imaging in mouse liver was also performed with both probes, but only the fluorescence of NIR-TrapG could be observed (Figure 9).

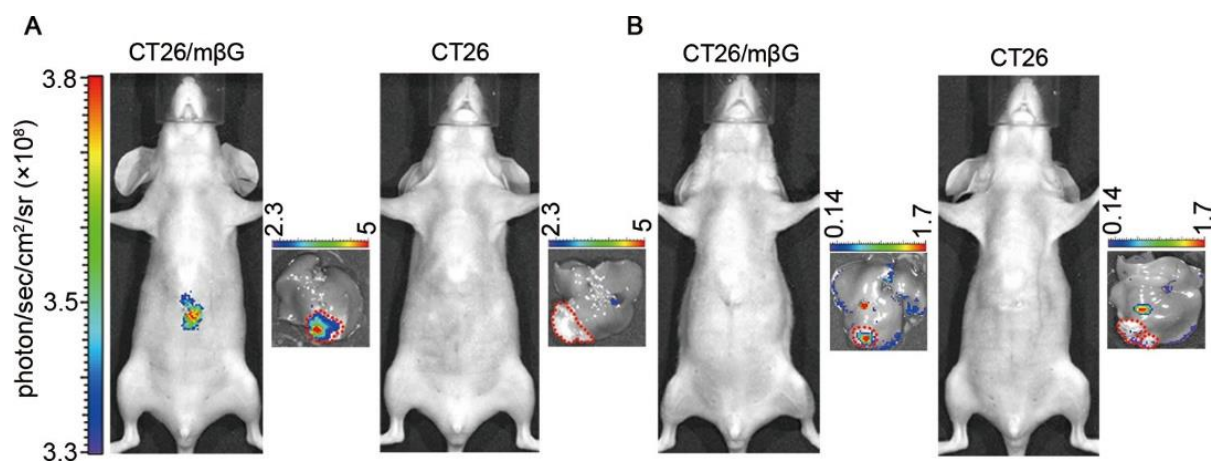


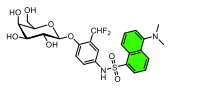
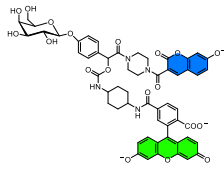
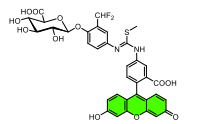
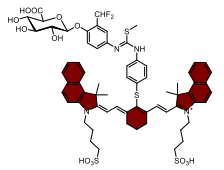
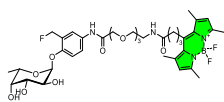
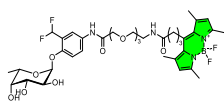
Figure 9. Imaging of CT26/m β G and CT26 cell-bearing mice with probes NIR-TrapG (A) and FITC-TrapG (B). Reprinted with permission from [50], copyright 2012 American Chemical Society.

Hsu et al. synthesized a useful tool for monitoring α -L-fucosidase activity [51]. The probes had the usual arrangement of the activity-based labeling agents, that is, an enzyme recognition head, a latent trapping unit, and a linker-bound reporter. A BODIPY derivative was responsible for the visualization, while the leaving groups *o*-fluoromethyl

and *o*-difluoromethyl moieties were applied. The probes were tested on a protein extract from *E. coli*, in which fucosidase was expressed: it was incubated for 1 h at four concentrations (5, 10, 20, 50 μM). Subsequent slot blot analysis resulted in weak fluorescence of the BODIPY ($\lambda_{\text{em}} = 520 \text{ nm}$) in case of the difluoromethylated residue and strong bands by the monofluorinated derivative. Labeling was performed at 10 μM concentration of the monofluorinated probe in AGS and HEK-293T cells: lysotracker showed the accumulation of probes in the lysosome, while the activity-dependence was also proven with the application of a fucosidase inhibitor. The authors also found a connection between *Helicobacter pylori* infection and increased α -L-fucosidase activity with the use of this probe [52].

For a summary of non-fluorogenic glycosidase probes, see Table 4.

Table 4. Non-fluorogenic activity-based probes for different glycosidases.

Structure ^a	Target Enzyme ^b	λ (nm) abs/em ^c	Notes	Studied System	Ref.
	GLB	360/520	inactivates GLB: <i>A. oryzae</i> : $K_i = 1.44 \text{ mM}$, $t_{1/2} = 10.5 \text{ min}$ bovine liver: $K_i = 0.22 \text{ mM}$, $t_{1/2} = 4.22 \text{ min}$ <i>B. circulans</i> : $K_i = 1.38 \text{ mM}$, $t_{1/2} = 11.2 \text{ min}$ <i>X. manihotis</i> : $K_i = 38.5 \text{ mM}$, $t_{1/2} = 21.1 \text{ min}$ <i>E. coli</i> : $K_i = 3.5 \text{ mM}$, $t_{1/2} = 4.3 \text{ min}$	in cellulose (B16 cells)	[44]
	GLB	400/515, 400/460	the ratiometric fluorescence response can be used for accurate determination of enzyme concentration; $k_{\text{cat}} = 6.1 \text{ s}^{-1}$, $K_M = 150 \mu\text{M}$	in cellulose (<i>LacZ</i> -positive HEK293 cells)	[47]
	GLB	490/525	no loss of enzyme activity, cross-labeling with other proteins, can be used for in vivo imaging of subcutaneous tumors	in vitro (<i>E. coli</i> and CT26), in vivo (mice)	[50]
	GLB	710/835	can be used for in vivo imaging of subcutaneous and deep tissue tumors	in vivo (mice)	[50]
	FUCA	497/520	efficient labeling, localizes in lysosomes, low cytotoxicity	in cellulose (AGS and HEK293 cells)	[51,52]
	FUCA	497/520	low labeling efficiency	in vitro	[51]

^a fluorophores are colored according to the approximate emission maxima. ^b enzyme abbreviations: GLB: β -galactosidase, FUCA: α -L-fucosidase. ^c approximate absorption and emission maxima.

Doura and coworkers developed a new class of fluorogenic substrates for the in vivo imaging of β -galactosidase activity displayed by *lacZ*(+) cells [53]. They modified an already existing substrate of β -galactosidase, the hydroxymethyl-bearing rhodol HMDER- β Gal [54]. The probes' fluorogenicity is quenched when its phenolic OH is substituted due to a preference for the spirocyclic form that has negligible fluorescence. Liberating the phenolate moiety restores the fluorescence. By substituting the OH with an enzyme substrate, fluorescence turn-on can indicate enzyme activity. A fluoro- or difluoromethyl moiety is incorporated to *ortho* position to the β -galactosidase substrate as a leaving group (SPiDER- β Gal-1 and -2) (Figure 10). In vitro study of the probes was in accordance with the earlier published observations, that is, SPiDER- β Gal-1 was more reactive than the SPiDER- β Gal-2 thus greater fluorescence turn-on could be detected (without other proteins, 650- and 210-fold, respectively). *LacZ* reporter, which is responsible for encoding *E. coli*

β -galactosidase enzyme, could be visualized in HEK cell lysates. Several rhodol-bound proteins were revealed by SDS-PAGE, but free nucleophiles, e.g., water, were also able to react with the QM. The advantage of the synthesized probes, especially SPiDER- β Gal-1, compared to HMDER is that they could distinguish *LacZ*(+) cells from *LacZ*(-) cells (Figure 10) without dissociating away from the active site, even under ex vivo conditions in *Drosophila* species and live mouse tissue.

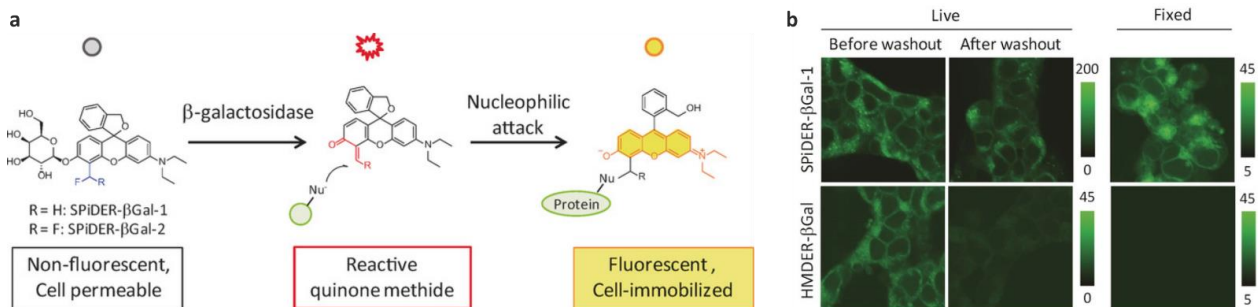


Figure 10. (a) Activation of SPiDER- β Gal-1 and -2. (b) SDS-PAGE visualization of SPiDER- β Gal-1 and -2 in comparison with HMDER- β Gal in HEK-*LacZ*(+) cells. (b) Fluorescent imaging of HEK-*LacZ*(+) cells incubated with either SPiDER- β Gal-1 or HMDER- β Gal (1 μ M). Before and after washing and after fixation with 4% paraformaldehyde. Adapted with permission from [53], copyright 2016 John Wiley and Sons.

A similar probe was developed for β -galactosidase activity, but with red-shifted fluorescence using silicon-rhodamine derivatives [55]. For preliminary experiments, the authors synthesized the 2'-Me-Sirhodol analogue (Figure 11a). The properties of 2'-Me-Sirhodol enabled the study of the probe at near physiological pH, because, according to its phenolic OH's pK_a value, at pH 7.4 the equilibrium shifted toward the deprotonated form, which is necessary for QM formation. This compound, however, did not show specific labeling of *LacZ*(+) cells. Further experiments pointed out that the extended π -conjugation reduced the reactivity of the QM. 2'-Hydroxymethyl-Sirhodol, which utilized intramolecular spirocyclization, and thus π -disconnection did not work as expected: it remained in spiroether form, even at higher pH values (above 10). To fine-tune the spirocyclization, next the 2'-COOH-Sirhodol (SPiDER-Red- β Gal, Figure 11b) was studied, which displayed pK_{cycl} value of 7.8, meaning nearly half of the probes existed in fluorescent form at pH 7.4. SPiDER-Red- β Gal, nonfluorescent at pH 7.4, could differentiate *LacZ*(+) HEK cells from *LacZ*(-) ones with high resolution and S/N ratio, without the leaking of the dye. Ex vivo imaging in *Drosophila melanogaster* and fixed mouse brain slices was also carried out with the same differentiation ability.

To develop this concept further, Chiba and coworkers also attempted the targeted ablation of *LacZ*(+) cells with a selenorhodol-based activity probe [56]. Targeted cell ablation, i.e., selectively destroying cells, can be accomplished with the application of small-molecular photosensitizers being active only as a result of enzyme activity. Such activatable photosensitizer was synthesized earlier [57], although the phototoxic products dissociating away from the target cells was a major problem. The designed probe, SPiDER-killer- β Gal (Figure 12), showed negligible fluorescence and no phototoxicity in the spirocyclic, β -galactose substituted form. Upon enzymatic hydrolysis, the QM was formed, and as the nucleophilic moieties attack it, the spiroether opens. This hydroxymethyl form exhibits efficient 1O_2 production upon irradiation. Measurements at different pH values revealed that SPiDER-killer- β Gal exists at pH 7.4 in the spirocyclic form, while without β -galactose the equilibrium is shifted toward the open form. The probe could differentiate between *LacZ*(+) and *LacZ*(-) HEK cells and caused concentration-dependent apoptosis, while incubating the cells without irradiation left them unchanged. These tendencies could be observed also in *Drosophila melanogaster* live culture tissue and epithelium, demonstrating the versatility of the described probe as an activatable photosensitizer.

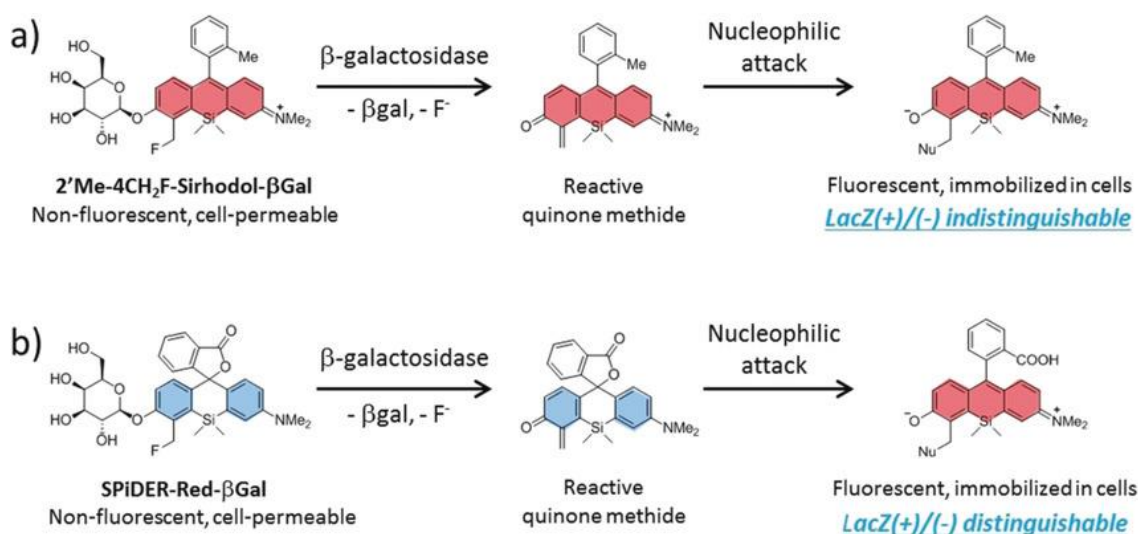


Figure 11. (a) Activation of nonfluorogenic 2'Me-4CH₂F-Sirhodol-βGal and (b) SPiDER-Red-βGal. Adapted with permission from [55], copyright 2018 John Wiley and Sons.

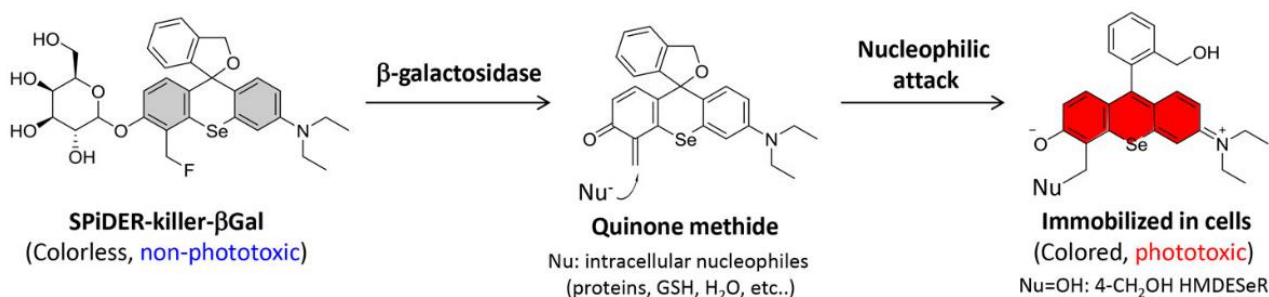


Figure 12. Activation of SPiDER-killer-βGal. Adapted with permission from [56], copyright 2019 American Chemical Society.

Inspired by Withers' work [49], Jiang and colleagues described a coumarin activated by β-galactosidase that utilized *p*-QM masked with a difluoromethyl group [58]. It was shown in previous examples that the difluoromethyl group can lead to the diffusion of the quinone methide resulting in lower labeling efficiency and weak fluorescence, but the authors hypothesized that moving the difluoromethyl group to the 3-position of the coumarin core would enhance the probe's properties (Figure 13a). This change in structure would probably generate a stronger fluorescent emission while diminishing steric hindrance towards the enzyme. The difluoromethylation was carried out by a photochemically-induced radical reaction from the corresponding coumarin (BGC-1) in one step, yielding the probe BGC-2. The new probe displayed a 60 nm bathochromic shift in the absorption wavelength compared to BGC-3, and had an over 200-fold fluorogenicity upon β-galactosidase activity. The emission spectrum of BGC-2 in PBS was similar to the 3-formylated coumarin derivative, revealing that a part of QM reacted with water instead of protein. SDS-PAGE experiments were also performed: the probe was incubated with β-galactosidase in the presence of BSA. According to fluorescent bands, both proteins were labeled. Live cell imaging was carried out in β-galactosidase, expressing CT26.CL25 cells and β-galactosidase-deficient CT.26WT cells (Figure 13b).

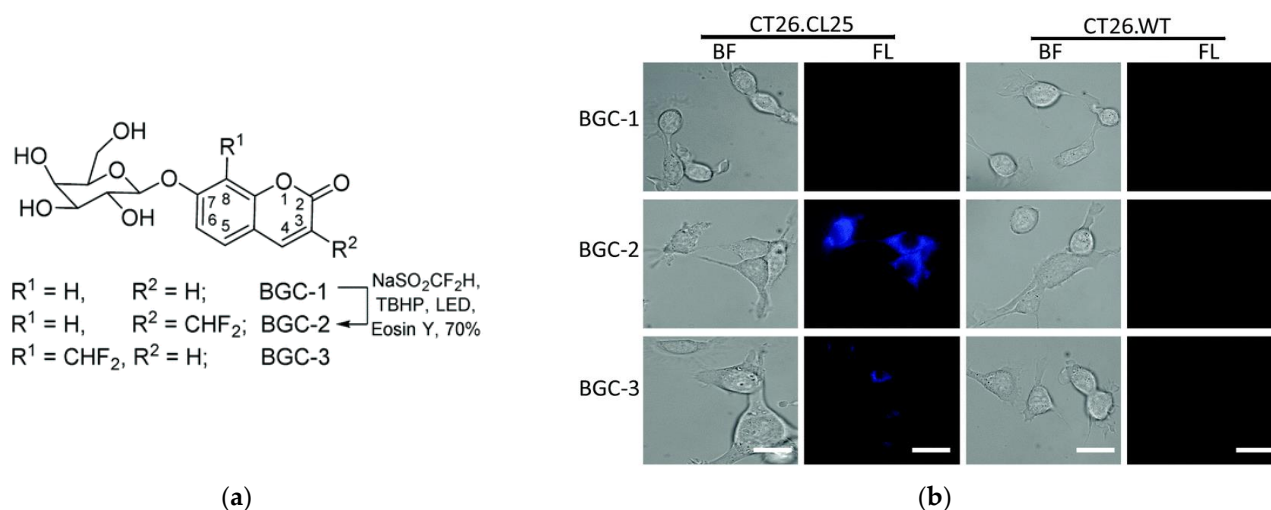


Figure 13. (a) Probes BGC-1, -2, and -3. (b) Fluorescent imaging in live CT26.CL25 and CT26.WT cells. Adapted from [58] with permission.

The monofluoromethyl-umbelliferon-galactoside [59] and SPiDER- β Gal [60] were also used in β -galactosidase-catalyzed fluorescence amplification methods for immunostaining.

Hyun and coworkers utilized the azide-alkyne click reaction to isolate different glycosidases [61]. Five coumarin probes were prepared that contained either a monofluoro- or difluoromethyl group for the QM masking, as well as an alkyne affinity tag. β -glucosidase, β -galactosidase, and β -*N*-acetylhexosaminidase substrates were applied. The authors envisioned that, after the immobilization of the coumarin probes, an added N₃-biotin reagent will undergo a click reaction with the alkyne moiety, and the subsequent affinity chromatography enables isolation of the enzymes. After reaction with their corresponding activity probes, the residual enzyme activity was determined with NIR-emitting activity probes. As a result, less of the monofluorinated derivative was needed (10 eq) for complete enzyme inactivation of enzymes than in the case of the difluorinated compounds (100 eq). Due to an undesired side reaction of the difluorinated probes upon ligation to the enzyme a weakly fluorescent adduct is formed, explaining the poorer labeling ability of said probes. The O-GlcNAcase activity was also monitored in HT-29 cells with great selectivity. The cell lysates were treated with N₃-biotin, followed by affinity chromatography yielding an isolated O-GlcNAcase. A similar probe with alkyne tag was developed for the monitoring of β -glucuronidase and bacterial α -L-fucosidase activity without a fluorescent reporter [62,63].

A senescence-associated β -galactosidase (SA- β -Gal) activatable NIR probe was developed by Liu et al. [64]. Senescence, that is, permanent cell growth arrest, is related with aging and age-related diseases. To detect this phenomenon *in vivo*, suitable NIR emitting fluorophores should be applied with a senescence-associated activation. To avoid dissociation of said dyes, a difluoromethyl leaving group was introduced to the designed NIR dyes (NIR-BG2, Figure 14). The monofluorinated derivative was also synthesized, however, it showed rapid decomposition via hydrolysis. The OH-group of the dye core is caged with the β -galactoside, connected through a self-immolative linker, quenching the fluorescence of the probe. Upon hydrolyzing NIR-BG2, only 16-fold fluorescence enhancement could be detected at 709 nm compared to the 100-fold turn-on of NIR-BG1 control without self-immobilizing properties. This difference could be attributed to quenching by formyl group formation via elimination of the second fluoride. NIR-BG2 was able to differentiate senescent HeLa cells from normal HeLa cells and *LacZ*(+) CT26.CL25 cells from CT26.WT cells. These cell imaging experiments pointed out the superiority of NIR-BG2 to NIR-BG1: the latter control probe could be washed out easily, while NIR-BG2 showed retained fluorescence. Camptothecin-induced cellular senescence in mice with HeLa tumor were also treated with NIR-BG2, with favorable outcomes.

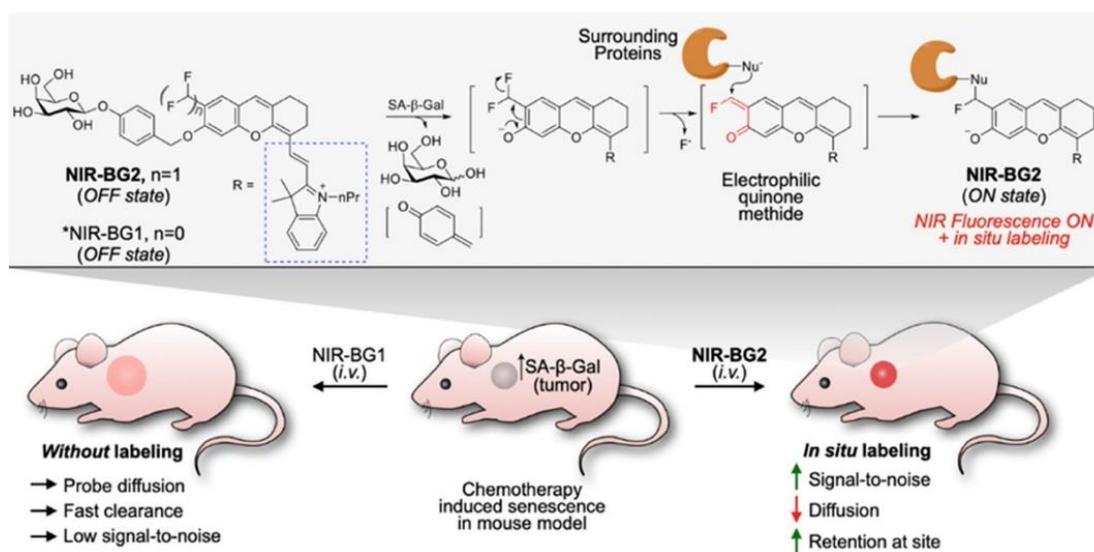


Figure 14. Activation of self-immobilizing probe NIR-BG2 and control probe NIR-BG1. Reprinted with permission from [64], copyright 2021 American Chemical Society.

For a summary of fluorogenic glycosidase probes, see Table 5.

Table 5. Fluorogenic activity-based probes for different glycosidases.

Structure ^a	Target Enzyme ^b	Turn-On Ratio	λ (nm) abs/em ^c	Notes	Studied System	Ref.
	NAGA	ND	490/520	used for the directed evolution of NAGAs: wild type: $k_{cat} = 384 \text{ s}^{-1}$, $K_M = 172 \text{ }\mu\text{M}$; variant: $k_{cat} = 287 \text{ s}^{-1}$, $K_M = 62 \text{ }\mu\text{M}$; cross-labeling with other proteins highly specific fluorescence labeling of the guard cells of stomata	in vivo (NovaBlue (D3) competent cells)	[48]
	GUSB	ND	330/450	no cytotoxicity in non-Abg encoding <i>E. coli</i> , moderate cytotoxicity in Abg encoding <i>E. coli</i> ; both probes can be used for cell sorting	in vivo (<i>Arabidopsis</i> (Col-0) plant)	[49]
	Abg/GB	ND	330/450	$k_{cat} = 3.38 \text{ s}^{-1}$, $K_M = 16.9 \text{ }\mu\text{M}$;	in cellulose (<i>E. coli</i> R1360 cells, <i>P. pastoris</i> cells)	[49]
	GLB	>650×	525/560	moderate cytotoxicity, better labeling efficiency than the difluoroderivative, cross-labeling with other proteins	in cellulose (HEK- <i>lacZ</i> (+) cells), ex vivo (<i>Drosophila melanogaster</i> and mice)	[53,60]
	GLB	>210×	525/560	$k_{cat} = 8.0 \text{ s}^{-1}$, $K_M = 29.6 \text{ }\mu\text{M}$; low labeling efficiency	in vitro	[53]

Table 5. Cont.

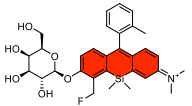
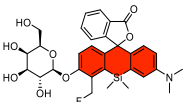
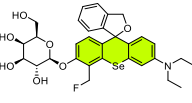
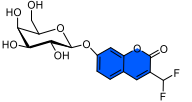
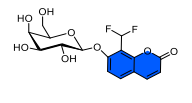
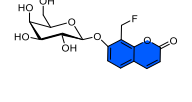
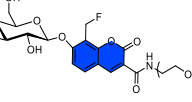
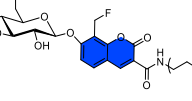
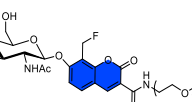
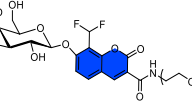
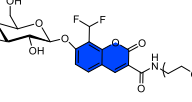
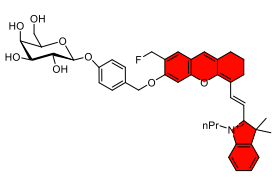
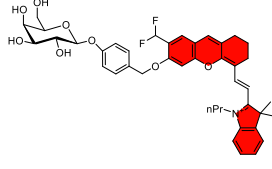
Structure ^a	Target Enzyme ^b	Turn-On Ratio	λ (nm) abs/em ^c	Notes	Studied System	Ref.
	GLB	>150×	610/630	reduced reactivity of the quinone-methide leads to leaking of the probe from the cells	in cellulose (HEK- <i>lacZ</i> (+) cells)	[55]
	GLB	>150×	610/630	cross-labeling with other proteins	in cellulose (HEK- <i>lacZ</i> (+) cells, ex vivo (<i>Drosophila melanogaster</i> and mice)	[55]
	GLB	NA ^d	525/560	modulated photosensitizer, selective ablation of <i>lacZ</i> (+) cells, $k_{cat} = 3.32 \text{ s}^{-1}$, $K_M = 10.1 \text{ }\mu\text{M}$ much higher fluorescence compared to the 8-difluoromethyl analogue, low cytotoxicity, cross-labeling with other proteins	in vitro (HEK- <i>lacZ</i> (+) cells, ex vivo and in vivo (<i>Drosophila melanogaster</i> and mice)	[56]
	GLB	>200×	416/454	low fluorescence upon hydrolysis by GLB	in cellulose (HEK- <i>lacZ</i> (+), HeLa and CT26.CL25 cells)	[58]
	GLB	ND	352/454	$k_{cat} = 54 \text{ min}^{-1}$, $K_m = 0.062 \text{ }\mu\text{M}$	in cellulose (HEK- <i>lacZ</i> (+) and CT26.CL25 cells)	[58]
	GLB	~200×	323/460	fluorescent detection of cell surface antigens using GLB labeled antibody	in cellulose (A549 cells)	[59]
	GLB	ND	330/450	inactivates the enzyme, no cross-labeling in cell lysate	in vitro	[61]
	GB	ND	330/450	inactivates the enzyme, no cross-labeling in cell lysate	in vitro	[61]
	HEX	ND	330/450	inactivates the enzyme, no cross-labeling in cell lysate low cytotoxicity the alkyne enables subsequent attachment of an affinity tag for protein isolation	in cellulose (HT-29 cells)	[61]
	GLB	ND	330/450	moderate enzyme inactivation, low labeling efficiency	in vitro	[61]
	GB	ND	330/450	moderate enzyme inactivation, low labeling efficiency	in vitro	[61]

Table 5. Cont.

Structure ^a	Target Enzyme ^b	Turn-On Ratio	λ (nm) abs/em ^c	Notes	Studied System	Ref.
	GLB	ND	650/710	hydrolyzes in buffer	in vitro	[64]
	GLB	16×	650/710	$k_{cat} = 14.6 \text{ s}^{-1}$, $K_m = 9.3 \text{ }\mu\text{M}$ more stable in buffer than the monofluoro derivative, low cytotoxicity	in cellulo (CT26.CL25, HeLa, MDA-MB-231, MCF7, IMR-90 cells), in vivo (mice)	[64]

^a fluorophores are colored according to the approximate emission maxima of the emissive form of the dye.

^b enzyme abbreviations: GLB: β -galactosidase, NAGA: α -N-acetyl-galactosaminidase, GUSB: β -glucuronidase, Abg: *Agrobacterium* sp. β -glucosidase/galactosidase, GB: β -glucosidase, FUCA: α -L-fucosidase, HEX: β -N-acetylhexosaminidase. ^c approximate absorption and emission maxima. ^d modulated photosensitizer

Neuraminidase (NA, also called sialidase) is one of the proteins encoded by viral RNA that can act as a key compound to understand viral infection. The evolution of neuraminidase activatable self-immobilizing probes started with Lu and coworkers' report [65]. The probe structure is similar to the earlier reported probes: a sialic acid enzyme substrate is connected to a trapping unit, having an *o*-difluoromethyl moiety and a biotin reporter. Tests carried out with NA obtained from *Arthrobacter ureafaciens* resulted in specific labeling of NA and without any labeling activity in the absence of the enzyme. Four different viral NA (from influenza A, *Arthrobacter ureafaciens*, *Clostridium perfringens*, *Vibrio cholerae*) were studied in the presence of the probe and zanamivir, a reversible inhibitor of NA activity, followed by residual activity determination with a methylumbelliferyl-substrate. Zanamivir acted as an effective inhibitor only in the case of influenza virus. The ELISA method was also conducted, and influenza A viruses were captured based on NA activity. With a modified version of the probe, containing a fluorescent dansyl unit instead of biotin, Hinou et al. studied *Vibrio cholerae* NA [66]. They showed that active site amino acids Asp-576 and Arg-577 were selectively labeled by the probe.

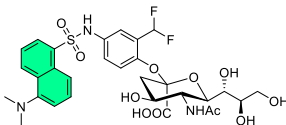
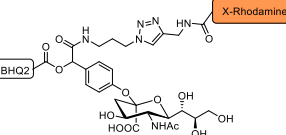
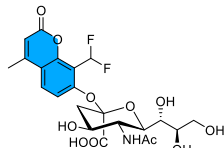
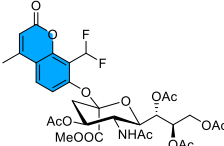
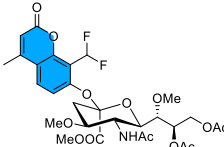
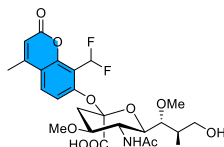
Zhu and colleagues used sialidase activatable self-immobilizing probes to deepen understanding on cellular senescence [67]. The probe had its features built up around a 4-hydroxymandelic acid core: sialic acid, as the recognition head; a rhodamine-X dye and a carbamate-linked blackhole quencher (BHQ). As long as the sialic acid substrate is intact, BHQ quenches the fluorescence of the rhodamine via FRET, but upon enzyme activation the carbamate bond is cleaved, and fluorescent emission is increased. An in vitro study with a recombinant neuraminidase was carried out, however, no fluorescent enhancement could be observed. This phenomenon could be attributed to covalent labeling of the enzyme and the subsequent activity loss. When the probe is hydrolyzed in the presence of BSA, both protein-dye conjugate can be visualized on SDS-PAGE, meaning that labeling is not specific on sialidase. Several live cell lines were incubated with the probe, but emission could be only observed in the case of sialidase-expressing cultures. They also did imaging of induced cellular senescence in human hepatocarcinoma Huh7 cells, which revealed lysosome-associated sialidase upregulation.

A probe with simpler structure was synthesized by Gao et al. [68]. Monitoring influenza virus neuraminidase activity was enabled by the sialic acid substrate, while ligation was made possible by a difluoromethyl coumarin dye. The fluorescent emission was detectable after several washing steps in *E. coli* labeling. MDCK cells, a host mammalian cell line for influenza growth, also recognized the sialidase substrate on the probe, however, in the presence of sialidase inhibitor, no fluorescent signal could be detected. When MDCK

cells were infected with H3N2 virus, the surviving cells also showed fluorescence increment. Upon treating these cells with a specific viral neuraminidase inhibitor, Oseltamivir, the subsequent addition of probe did not result in fluorescence emissions, that is, the developed probe was activatable by viral neuraminidase as well. To improve this selectivity towards viral sialidase, two methyl groups were introduced to the C4 and C7 hydroxyl groups. This probe showed no affinity to label uninfected MDCK cells, but exhibited intensive fluorescence by the H3N2 infected cell line.

For a summary of neuraminidase probes, see Table 6.

Table 6. Activity-based probes for neuraminidases.

Structure ^a	Turn-On Ratio	λ (nm) abs/em ^b	Kinetics	Notes	Studied System	Ref.
	NA	ND	$K_i = 1.90$ mM $t_{1/2} = 2.83$ min	inactivates the enzyme	in vitro	[66]
	110×	580/610	ND	cross-labeling with other proteins	in cellulo (A549, HeLa, HepG2, MCF-7, U2OS, Huh-7)	[67]
	ND	360/470	$K_M = 2.4$ μ M ^c	cannot differentiate endogenous MDCK sialidase and viral sialidase	in cellulo (MDCK cells)	[68]
	ND	360/470	ND	lower fluorescence in cellulo compared to the deacetylated probe	in cellulo (MDCK cells)	[68]
	ND	360/470	ND	only hydrolyzed by viral sialidase, lower fluorescence in cellulo compared to the deacetylated probe	in cellulo (MDCK cells)	[68]
	ND	360/470	$K_M = 159$ μ M ^d	only hydrolyzed by viral sialidase	in cellulo (MDCK cells)	[68]

^a fluorophores are colored according to the approximate emission maxima of the emissive form of the dye. ^b approximate absorption and emission maxima. ^c determined using NedA *Micromonospora viridifaciens*. ^d determined using H3N2 (A/Hong Kong /1/68) neuraminidase.

3.3. γ -Glutamyl-Transpeptidase

The first QM-based activity probe for γ -glutamyl transpeptidase (GGT) was developed by Li and colleagues [69]. This enzyme is capable of catalyzing γ -glutamyl bond cleavage, and its increased activity can be associated with malignant tumors, thus selective labeling would benefit therapeutic applications. The structure of the probe (GGTIN-1, Figure 15) consists of γ -Glu, a self-immolative *p*-aminobenzyl linker, a HD-NIR dye containing a zwitterionic moiety, and the rarely utilized ethyl carbamate leaving group. When 10 μ M

GGTIN-1 solution was treated with GGT in PBS at 37 °C for 30 min, the fluorescence intensity was weaker than that of the control GGTIN-0, which can be attributed to the lack of nucleophiles in vitro. This intensity, however, was increased upon β -mercaptoethanol addition corresponding to the SH-bound dye. SDS-PAGE analysis showed that multiple proteins, such as GGT and BSA, present in the system are labeled after the activating trigger. Live HEPG2 cells and U87MG cells, known to overexpress GGT, were also incubated with GGTIN-1: real-time imaging was performed with no-wash conditions (Figure 15). In vivo imaging of mice with xenografted U87MG tumor was also feasible, and the intensive fluorescent emission was detectable even after 24 h. Organs of the mice were also analyzed as showing strong liver- and kidney-originated emission, proving increased GGT activity.

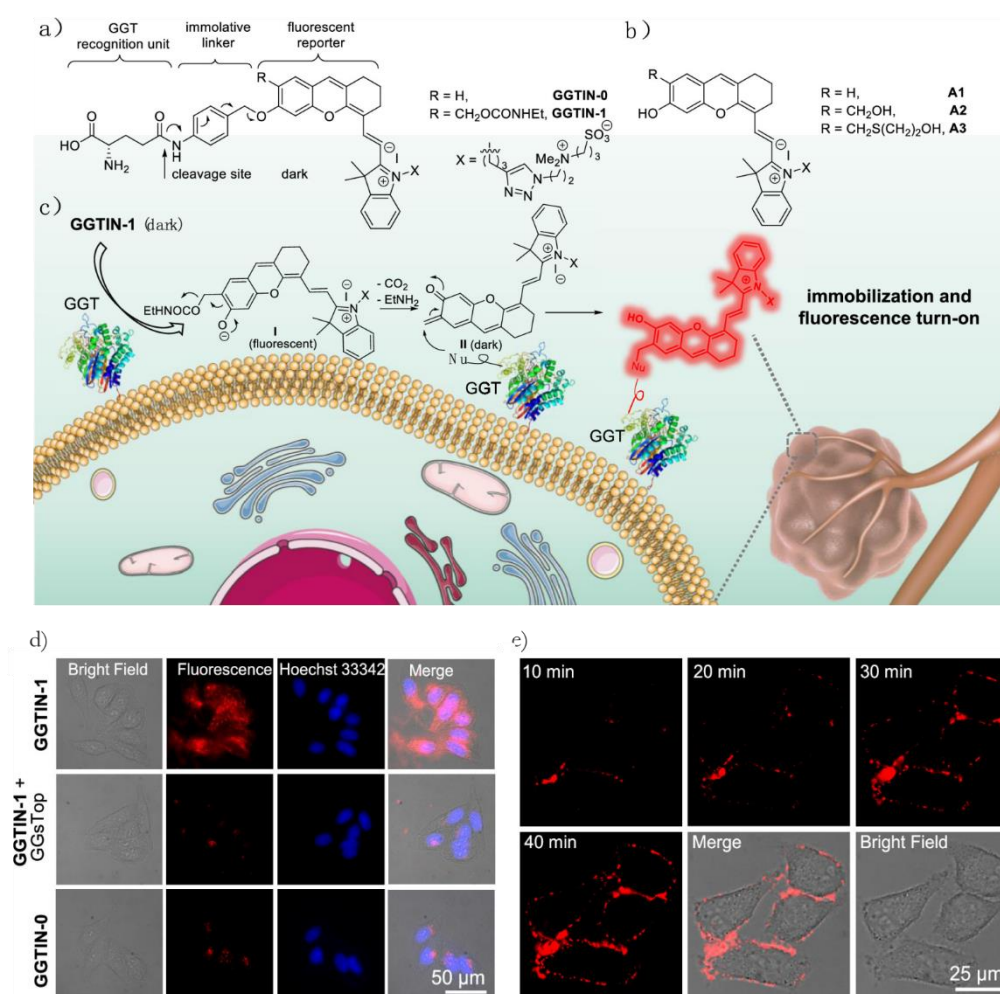


Figure 15. (a) Structures of GGTIN-0, GGTIN-1, (b) A1, A2, and A3. (c) Turn-on mechanism activated by γ -glutamyl transpeptidase. (d) Fluorescent imaging of γ -glutamyl transpeptidase activity in HepG2 cells or GGsTop (0.5 mM), a γ -glutamyl transpeptidase inhibitor pretreated HepG2 cells with GGTIN-0 and GGTIN-1 (5 μ M, 37 °C, 1 h incubation). (e) Real-time and wash-free images obtained with the use of GGTIN-1. Reprinted with permission from [69], copyright 2020 American Chemical Society.

A rhodamine-based fluorescent GGT activity probe was described as well [70]. γ -Glu and a fluoromethyl group were introduced to a hydroxymethyl diethylrhodamine (4-CH₂F-HMDiEtR-gGlu), which was capable of binding to nucleophiles via aza-QM formation. Intramolecular spirocyclization was utilized for tuning the pH dependence of the probe's photophysical properties, while the absorbance of 4-CH₂F-HMDiEtR-gGlu was reduced ($pK_{cycl} = 5.4$), meaning that it existed in a colorless, spirocyclic form at pH 7.4, and 4-

CH₂OH-HMDiEtR-gGlu mainly displayed strong fluorescence ($pK_{cycl} = 9.6$). Incubating the probe with GGT in vitro did not result in loss of enzyme activity. Live cell imaging was carried out on SHIN3 cells displaying high GGT activity and SKOV3 cells (Figure 16) with low GGT activity. A comparative study was done with gGlu-HMRG, an activity probe of GGT which is not capable of self-immobilization. This latter dye stained both type of cells, while applying 4-CH₂F-HMDiEtR-gGlu resulted in specific emission. In vivo imaging on SHIN3 bearing mice showed the same outcome.

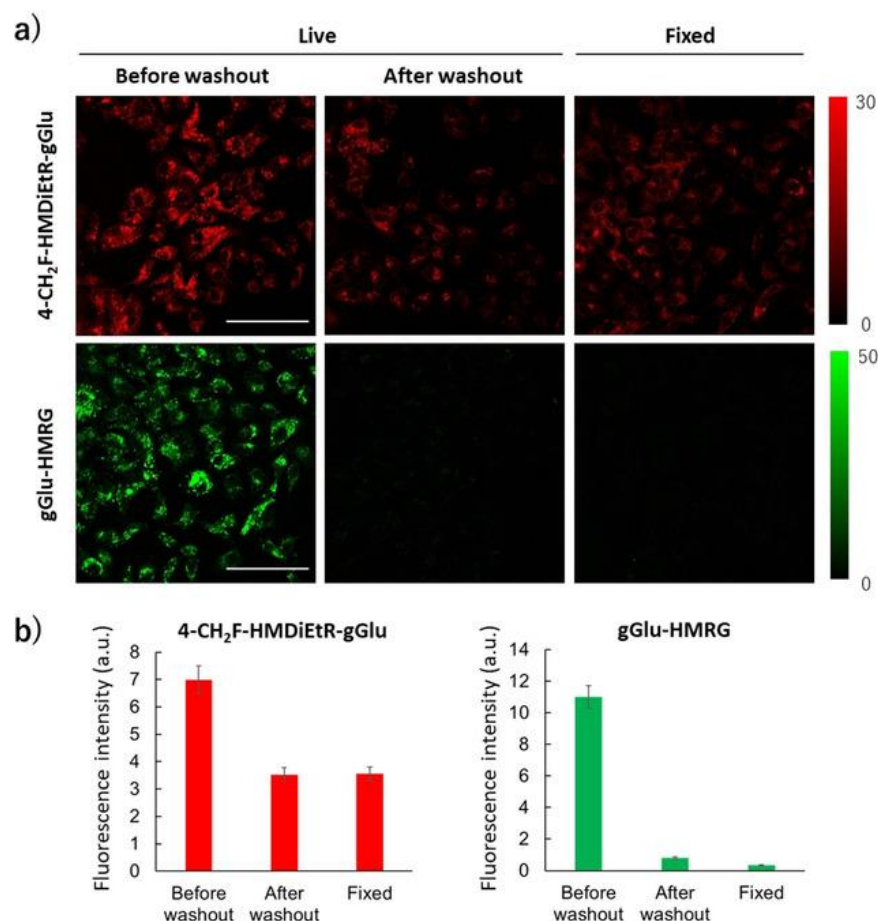


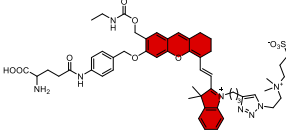
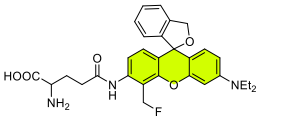
Figure 16. (a) Fluorescent imaging of γ -glutamyl transpeptidase activity in SHIN3 cells with 4-CH₂F-HMDiEtR-gGlu and non-immobilizable gGlu-HMRG (1 μ M) before washing, after washing, and after fixation with 4% paraformaldehyde. (b) The measured fluorescent intensity. Reproduced with permission from [70], copyright 2020 John Wiley and Sons.

For a summary of γ -glutamyl-transpeptidase probes, see Table 7.

3.4. Sulfatases

Analogous to the phosphatase family, sulfatases play a crucial role in many biochemical pathways by removing the sulfate group from various molecules. The first activity-based probe for sulfatases was demonstrated by Lu and coworkers [71]. The authors designed an aryl-sulfate recognition head connecting to the latent trapping unit (from *p*-monofluoromethyl group, *p*-QM formation is expected) to which a biotin is attached. The probe, selective for steroid sulfatase (STS), was studied with human STS expressed in CHO-K1 cells. After binding to streptavidin affinity gel surface, the probe was injected with STS fractions, and the conjugates were isolated and examined with SDS-PAGE. Visualization with anti-STs antibody showed that specific labeling was successful. No labeling was observed in the presence of estrone-3-O-sulfamate, a potent inhibitor of STS, which is in line with activity-dependent behavior.

Table 7. Activity-based probes for γ -glutamyl-transpeptidase.

Structure ^a	Turn-On Ratio	λ (nm) abs/em ^b	Notes	Studied System	Ref.
	40 ×	690/715	cross-labeling with other protein, no cytotoxicity	in cellulo (HepG2, U87MG) in vivo (mouse)	[69]
	>500 ×	530/565	cross-labeling with other protein, no loss of enzyme activity	in cellulo (SHIN3 A549, MIA PaCa-2, HepG2) in vivo (mouse)	[70]

^a fluorophores are colored according to the approximate emission maxima of the emissive form of the dye.

^b approximate absorption and emission maxima.

Lenger and colleagues accomplished more precise sulfatase-based labeling with the utilization of a fluorescent dye reporter [72]. The authors aimed to improve probes 1 and 2, which displayed poor selectivity and did not act as irreversible and selective inhibitors of sulfatases (Figure 17). By designing probes 3 and 4, the more reactive monofluorophenyl group enabled better labeling efficiency (Figure 17). The probes were tested on four different sulfatases, two bacterial aryl sulfatases (KARS and PARS), one human aryl sulfatase (ARSG), and steroid sulfatase. The retained enzyme activity was determined with pNCS, a chromogenic (KARS, PARS, ARSG), or ³DHEAS, a radioactive sulfatase substrate (STS). Model compound 3 showed significant inactivation rate of KARS after 30 min (50%, 0.8 μ M), but with the exception of ARSG, which was not affected at all, the inhibition happened in a time- and concentration-dependent manner in all cases. To determine the turnover ratio, a labeling experiment was conducted over 2 weeks, where the concentration of the probe and KARS was 140 μ M and 70 nM, respectively. For the inactivation of every enzyme molecule 400 molecules of probe 3 were needed, which is in agreement with the earlier observations. Finally, crude *E. coli* lysates, which contained either active, inactive, or no sulfatase, were incubated with 1 mM probe 4, and the subsequent SDS-PAGE separation was followed by fluorescent imaging. It was shown that probe turnover was enzyme activity-dependent, however, the subsequent labeling was nonspecific.

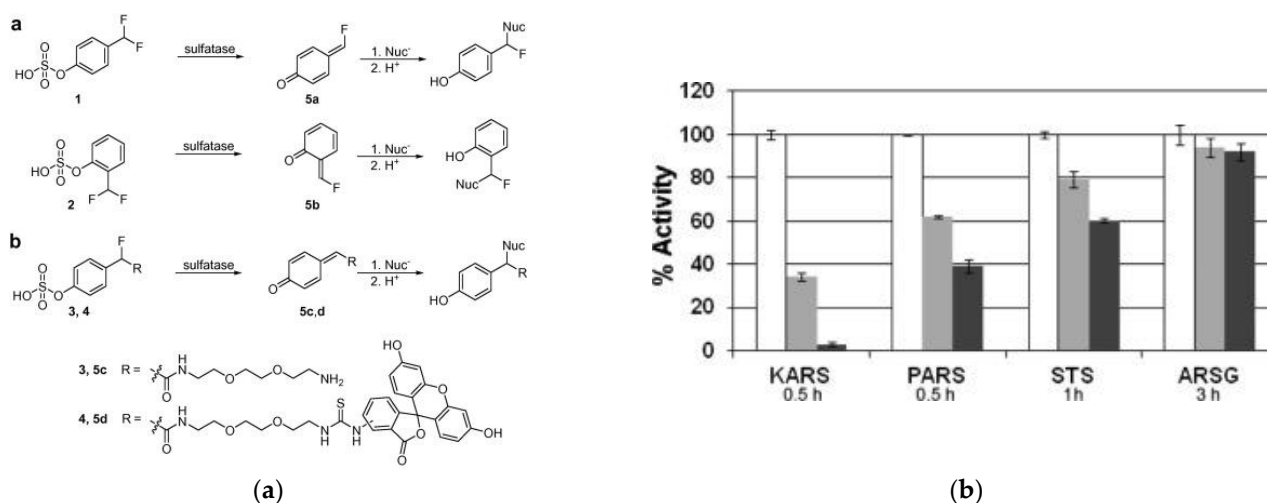


Figure 17. (a) Activation of probes 1–4 by sulfatase activity. (b) Inhibition of the four sulfatases (white: without inhibitor, grey: 1 mM inhibitor, black: 3 mM inhibitor). Reproduced with permission from [72], copyright 2012 Elsevier.

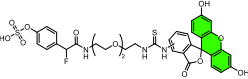
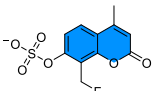
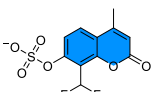
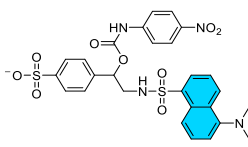
Steroid sulfatase activity-based probes containing the substrate directly on the dye core were also synthesized [73]. A fluorogenic coumarin frame, with either monofluoromethyl or difluoromethyl groups in the 8-position, had its phenolic OH caged by a sulfate group. The probes displayed a similar enzyme inactivation rate, with STS preparations verified by ^{19}F NMR measurements: 25–30% hydrolysis of probes was enough to reach nearly complete enzyme inhibition. Next, 50 μg CHO/STS cell lysates were incubated with the probes (5 μM) in TRIS buffer. In the case of the monofluorinated derivative, 465 nm emission was detected upon incubation for 2 h showing a 7-fold increment. No fluorescence enhancement was detected by the difluorinated probe.

Intramolecular fluorescence quenching was also utilized in sulfatase activatable probes [74]. To the 4-(hydroxymethyl)phenyl-core a sulfate substrate, a dansyl fluorescent reporter and a *p*-nitrophenyl group were attached, the latter through a carbamate linker. Upon commercially available arylsulfatase activity, the carbamate bond was cleaved, and liberation of *p*-nitrobenzylamine moiety leads to restored dansyl emission at 480 nm.

Competitive labeling experiments proved that labeling with the probe caused partial loss of enzyme activity. To confirm that the probe is attached to the target enzyme, SDS-PAGE analysis was also carried out. Although the probe was not highly efficient, it formed a covalent conjugate with sulfatase.

For a summary of sulfatase probes, see Table 8.

Table 8. Activity-based probes for different sulfatases.

Structure ^a	Target Enzyme	Turn-On Ratio	λ (nm) abs/em ^b	Notes	Studied System	Ref.
	PARS KARS STS	NA	490/520	inactivates PARS, KARS and STS, ARSG not affected; cross-labeling in cell lysate	in vitro	[72]
	STS	7 \times	360/465	inactivates STS, cross-labeling not studied	in cellulo (CHO/STS)	[73]
	STS	NA	360/465	hydrolyzed by STS, but non-fluorescent side product both in vitro and in cellulo	in cellulo (CHO/STS)	[73]
	Sulfatase from <i>Aerobacter aerogenes</i>	5 \times	330/480	cross-labeling not studied	in vitro	[74]

^a fluorophores are colored according to the approximate emission maxima of the emissive form of the dye.

^b approximate absorption and emission maxima.

3.5. β -Lactamases

Imaging bacterial antibiotic resistance through β -lactamase-associated methods would propel drug development greatly. Shao and coworkers designed FRET systems that are capable of covalently labeling antibiotic resistant bacteria [75]. Figure 18 shows the arrangement of such systems: to a *p*-hydroxybenzyl moiety, an oxidized cephalosporin substrate group, a fluorescent dye, and a fluorescence quencher were attached. The quencher was chosen to correspond to the requirements of FRET, so its absorption spectrum must overlap with the dye's emission spectrum. Accordingly, quenching pairs were designed with FITC, Cy3 and Cy5.5 dyes with dabcy1, BHQ2, and BHQ3 quenchers, respectively. As soon as the bacteria hydrolyses the cephalosporin, the ester bond is cleaved, liberating the quencher.

Upon TEM-1 β -lactamase addition in PBS buffer, the fluorescence enhancement was 38-, 110-, and 80-fold for LRBL1, -2, and -3, respectively. SDS-PAGE experiments confirmed the covalent ligation of the dyes to the target enzyme, while MALDI-TOF analysis showed that multiple modifications occurred on one enzyme. As a result of live cell imaging, carried out on Gram negative penicillin resistant *E. coli* and antibiotic susceptible *E. coli*, specific labeling was observed with strong fluorescence and high signal-to-noise ratio. Based on this, separation of the two types with flow cytometry was also possible compared to the problematic application of conventional dyes.

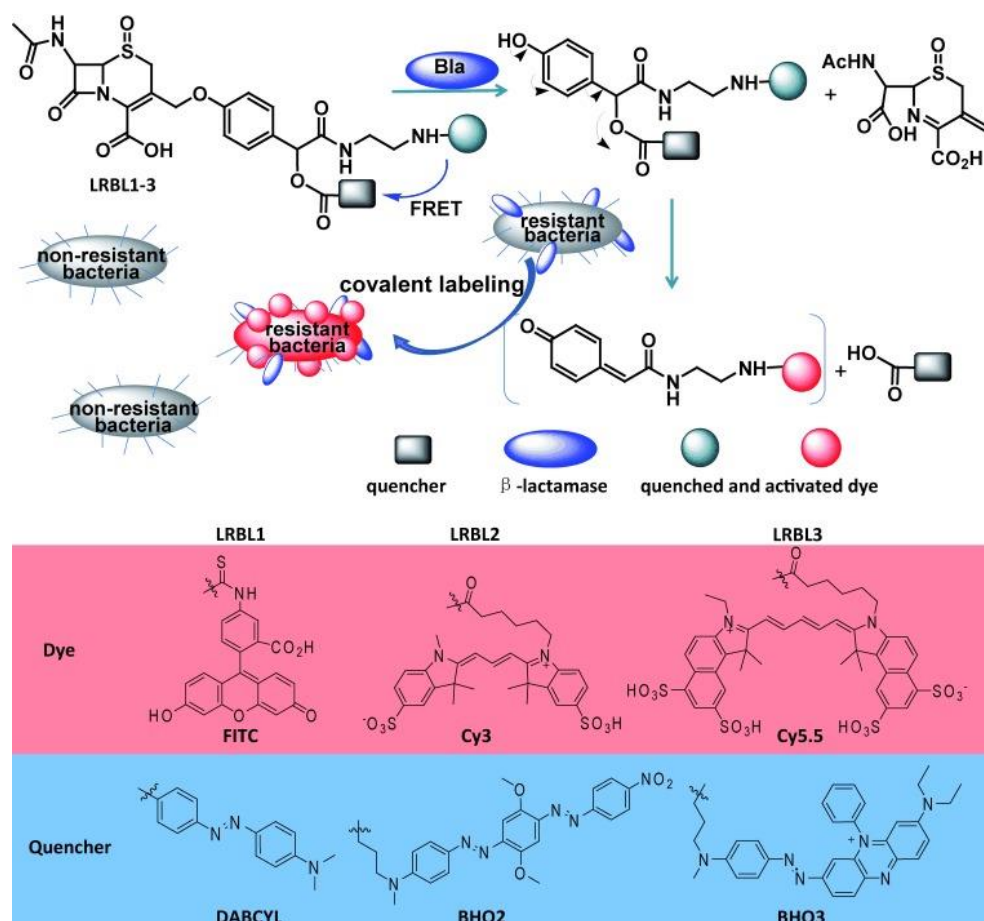
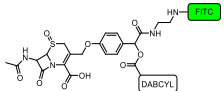
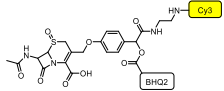
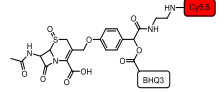
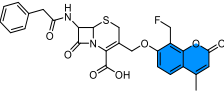
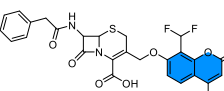


Figure 18. Activation of probes LRBL1, LRBL2, and LRBL3 by antibiotic-resistant bacteria and applied fluorophores and quenchers. Reproduced with permission from [75], copyright 2013 John Wiley and Sons.

A coumarin was also utilized in activity-based β -lactamase detection [76]. In the 8-position, mono- and difluorinated derivatives were described, with a β -lactamase substrate caging the fluorescence of the dye. The monofluoro-containing probe exhibited a 50-fold fluorescent enhancement upon TEM-1 addition to β -lactamase in buffer, while the difluorinated one showed intense fluorescence only after the addition of effective nucleophiles as well. On the other hand, the difluoro-probe showed better labeling efficiency according to SDS-PAGE analysis. This phenomenon can be attributed to reaction with water in case of the monofluorinated probe. The specificity of the difluoro-probe was also better: in the presence of BSA it showed mainly covalent ligation to the target enzyme. In imaging of TEM-1 coding *E. coli* bacteria, the difluoro-dye performed better as well. Three more pathogenic bacteria strains were studied with the same outcome.

For a summary of β -lactamase probes, see Table 9.

Table 9. Activity-based probes for β -lactamases.

Structure ^a	Turn-On Ratio	λ (nm) abs/em ^b	k_{cat} (min ⁻¹)	K_M (μ M)	Notes	Studied System	Ref.
	38×	490/520	4.92	3.08	no loss of enzyme activity, cross-labeling not studied	in cellulo (<i>E. coli</i> , <i>B. cereus</i> , MRSA, <i>S. aureus</i>)	[75] ^c
	110×	525/570	2.16	4.28	no loss of enzyme activity, cross-labeling not studied	in cellulo (<i>E. coli</i> , <i>B. cereus</i> , MRSA, <i>S. aureus</i>)	[75] ^c
	80×	650/680	1.49	5.24	no loss of enzyme activity, cross-labeling not studied	in cellulo (<i>E. coli</i> , <i>B. cereus</i> , MRSA, <i>S. aureus</i>)	[75] ^c
	50×	365/460	ND	ND	hydrolyzed by β -lactamase but weak fluorescence in cellulo	in cellulo (<i>E. coli</i>)	[76]
	<50×	365/460	ND	ND	cross-labeling not studied	in cellulo (<i>E. coli</i> , MDR <i>A. baumannii</i> , <i>K. pneumoniae</i>)	[76]

^a fluorophores are colored according to the approximate emission maxima of the emissive form of the dye.

^b approximate absorption and emission maxima. ^c for details of the structures, see Figure 18.

3.6. Other Enzymes

Although activity-based probes most frequently target the aforementioned enzyme types, examples of labeling others are not without precedent. Carboxylesterases (CXE), that is, a group of serine hydrolases, could be targeted with Sellars and coworkers' probe [77]. They utilized the fluorescence quenching effect displayed by *p*-nitrophenyl group that is connected via an easily fragmentable carbamate bond to the 4-hydroxymandelic acid core. A dansyl group was applied as fluorescent reporter, while *p*-hydroxybenzylic ester moiety served as enzyme substrate. Quenching resulted in a decreased fluorescent quantum yield of 8% compared to the 89% displayed by the non-quenched dye. Hydrolysis with KOH leads to 6-fold fluorescent increment. The authors then applied purified recombinant *AtCXE12* serine hydrolase (0.8 mg/mL) to activate the probe (10 mM): at 37 °C and pH 7.4 3 h were needed for complete conversion. SDS-PAGE visualization revealed that multiple dyes were attached to one enzyme molecule in two regions.

Esterase targeting, acetyl-containing probes were synthesized by Shi and colleagues [78]. DHA, that is, diacetylated 4-hydroxymandelate, was chosen as core, in which the acetyl group on the aromatic ring acts as a substrate, while the other will be the leaving group. The applicability of such systems was demonstrated with sodium methoxide as a reaction partner: acetyl leaving also led to QM formation. Coumarin, fluorescein, and rhodamine were attached to the core, enabling fluorescent detection. The dyes exhibited selective labeling towards porcine liver esterase in the presence of BSA. Imaging in HeLa cells showed that the probe was captured by proteins in close proximity to the enzyme. The probes were able to track dying cells as well: they were activated and labeled by a receptor-interacting protein 3 that was followed by induced apoptosis.

The presence of nitroreductase (NTR) can indicate hypoxia tumor environment, thus detecting its activity can benefit therapeutic applications. To avoid the diffusion from the active site, a red emitting ($\lambda_{em,max} = 560$ nm) hemicyanine-based probe was designed recently by Wang and coworkers, utilizing QM chemistry (FY, Figure 19a) [79]. After the enzyme finds the recognizable unit, the aromatic or heterocyclic moiety containing a nitro group, a QM is formed as a result of reduction and subsequent electronic rearrangement (Figure 19). The applied *p*-nitrobenzyl group possessed a dual role: it was not only used as a recognition unit for nitroreductase but also as a quencher of the hemicyanine's fluorescence

by internal charge transfer processes. Live cell labelling was performed in normal cells (HEK293T) and cancer cells (A549), and the probe displayed good selectivity and sensitivity for NTR in mitochondria. Labeling on A549 cells both live and after fixation showed a significant difference between normoxic and hypoxic environments and the lack of labeling with the application of NY, a probe without the fluoromethyl substitution (Figure 19b). The feasibility of the designed system was demonstrated by zebrafish labelling as well.

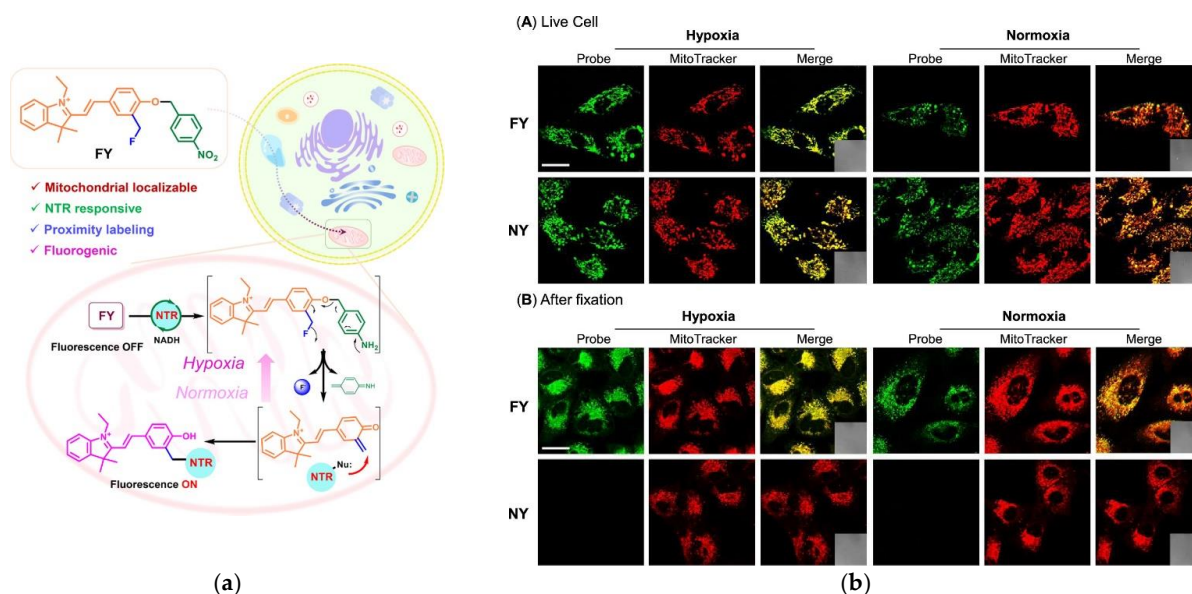


Figure 19. (a) FY probe and its activation. (b) Fluorescent imaging of FY/NY probes in live A549 cells ($c_{\text{probes}} = 20 \mu\text{M}$) and after MeOH fixation ($c_{\text{probes}} = 100 \mu\text{M}$). Reprinted with permission from [79], copyright 2022 American Chemical Society.

For a summary of probes for other enzymes, see Table 10.

Table 10. Activity-based probes for other enzymes.

Structure ^a	Target Enzyme	Turn-On Ratio	λ (nm) abs/em ^b	Notes	Studied System	Ref.
	AtCXE12	10×	335/540	cross-labeling with <i>Ta</i> GSTL1 having a reactive Cys residue, no cross-labeling with BSA	in vitro	[77]
	esterase	NA	375/445	low cytotoxicity, cross-labeling not studied	in cellulo (HeLA, 3T3, A549, B16F10, Huh-7, U2OS and Raw 264.7)	[78]
	esterase	NA	495/520	low cytotoxicity, cross-labeling not studied	in cellulo (HeLA, 3T3, A549, B16F10, Huh-7, U2OS and Raw 264.7)	[78]
	esterase	NA	550/575	low cytotoxicity, in cellulo cross-labeling	in cellulo (HeLA, 3T3, A549, B16F10, Huh-7, U2OS and Raw 264.7)	[78]
	nitro-reductase	10×	520/560	low cytotoxicity, no cross-labeling	in cellulo (A549) in vivo (zebrafish)	[79]

^a fluorophores are colored according to the approximate emission maxima of the emissive form of the dye.

^b approximate absorption and emission maxima.

3.7. Reactive Oxygen Species (ROS)

Reactive oxygen species (ROS) are unstable oxygen-containing molecules or radicals (e.g., peroxides, hydroxide radical, singlet oxygen) that assist in the damage of biomolecules and subsequent cell death. H_2O_2 -mediated QM formation was studied earlier by tuning arylboronate recognition moiety, although applying fluoride as the leaving group has been without precedent in these early works [80–82]. A H_2O_2 responsive, QM-based probe containing a boronate trigger was designed by Zhu and coworkers [83], utilizing a monofluoromethyl leaving group. The cleavage of the pinacolboronate group and the subsequent HF elimination led to *o*-QM formation that was able to attach a coumarin or a fluorescein in proximity to ROS activity. In vitro labeling with coumarin-containing Hyp-L-1 was carried out in the presence of BSA that exhibited intensive fluorescent signal upon H_2O_2 addition. However, not only H_2O_2 but peroxyxynitrite anion (ONOO^-) could also activate the probe. For live cell imaging on RAW264.7 macrophage Hyp-L-2 bearing a fluorescein dye was applied (Figure 20). Cellular uptake was ensured by the two acetyl groups attached to the phenolic OHs. Several fluorescent bands with different molecular weight could be visualized indicating high reactivity towards several nucleophiles. Without H_2O_2 , no fluorescence could be detected. Cells with chemically-induced ROS could be selectively differentiated from non-stimulated cells, and furthermore, mitochondria oxidative stress was also visualized. Stimulated oxidative stress was also observable in mouse brain tissue.

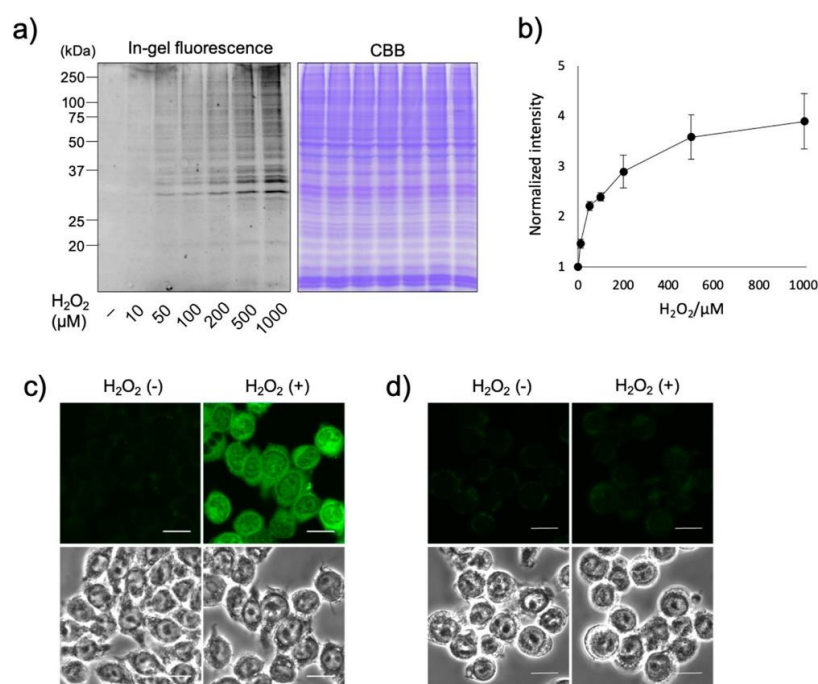


Figure 20. (a) SDS-PAGE analysis of Hyp-2-L (5 μM) labeling in living RAW264.7 cells with increasing H_2O_2 concentrations. (b) Normalized fluorescence intensity gained from the former labeling. (c) Fixed cells after Hyp-2-L treatment. (d) Images obtained with HYDRO-P, a commercially available H_2O_2 sensor, show low fluorescent on untreated cells. Reprinted with permission from [83], copyright 2020 American Chemical Society.

Another fluorescein-based H_2O_2 -responsive probe was reported by Iwashita and colleagues [84]. Peroxy Green-1 Fluoromethyl (PG1-FM) can sense H_2O_2 via its boronate group, while the incorporated monofluoromethyl group provides the masked QM. When the boronate group is intact, the dye exists in spirocyclic form, which enables cell permeability. Upon reaction with cellular H_2O_2 , proximity labeling of proteins or water occurs through QM formation and the forming fluorescent dye, in its open form, will become membrane-impermeable. The probe was tested in vitro at physiological pH with multiple

ROS, but showed only selective labeling upon H_2O_2 activity, even compared to peroxy-nitrite. The addition of BSA and MFP 231 cell lysates resulted in labeled proteins, showing no selectivity in covalent ligation. Exogenously H_2O_2 -treated HeLa cells were also studied, and the probe showed minimal cytotoxicity during labeling. Endogenous H_2O_2 production, triggered by paraquat treatment in HeLa cells, growth factor stimulation in A431 cells, and PMA treatment in RAW 264.7 macrophages, was also monitored. In all cases, fluorescent enhancement could be detected with minimal background signal, while the lack or quenching of H_2O_2 did not yield any fluorescent response. The ability to detect peroxide was also demonstrated in a microglia-neuron coculture.

Novel ROS sensing agents with a quaternary ammonium salt leaving group were designed by Jung and coworkers [85]. As demonstrated before, both monofluoro- and difluoromethyl caging of QM function have drawbacks: the former can be unstable and prone to hydrolysis in aqueous solutions, while the slow QM formation from the latter allows the probe to diffuse away from activation site. Furthermore, the diethylaminosulfur trifluoride (DAST) that is most frequently used for fluorine incorporation is a toxic, sensitive, and expensive reagent. The authors attempted to overcome these challenges by applying a morpholinium salt as a leaving group. To study the release process and choose the suitable fluorescent dyes, several morpholinium substituted model fluorophores, such as naphthylimide, coumarin, acedan, rhodol, and benzorazol, were synthesized containing a light-cleavable *o*-nitrobenzyl group (Figure 21). These probes are supposed to be activated by UV-light irradiation. Until the *p*-nitrobenzyl group is intact, no emission is exhibited by the dye due to PET quenching, except for the benzorazol derivative. Fluorescent enhancement could be observed upon light irradiation, the generated species labeled BSA rapidly at pH 7.4 in PBS buffer. The authors performed a labeling experiment in the presence of Boc-protected amino acids Lys, Cys and Ser, concluding that the probes were mainly attached to the thiol group of Cys. The naphthylimide derivative was also tested in HeLa cells: the fluorescence of the probe was retained even after the wash-out step. As the model compounds seem to work as expected, ROS/RNS activatable analogue was synthesized from the naphthylimide core by introducing an arylboronate instead of *p*-nitrobenzyl. H_2O_2 , peroxy-nitrite, superoxide, hydroxy radical, and singlet oxygen were able to trigger fluorescent response and label BSA accordingly. Exogenously added and endogenously triggered H_2O_2 yielded strongly fluorescent cellular proteins, and the presence of ROS could be detected in mouse kidney tissue.

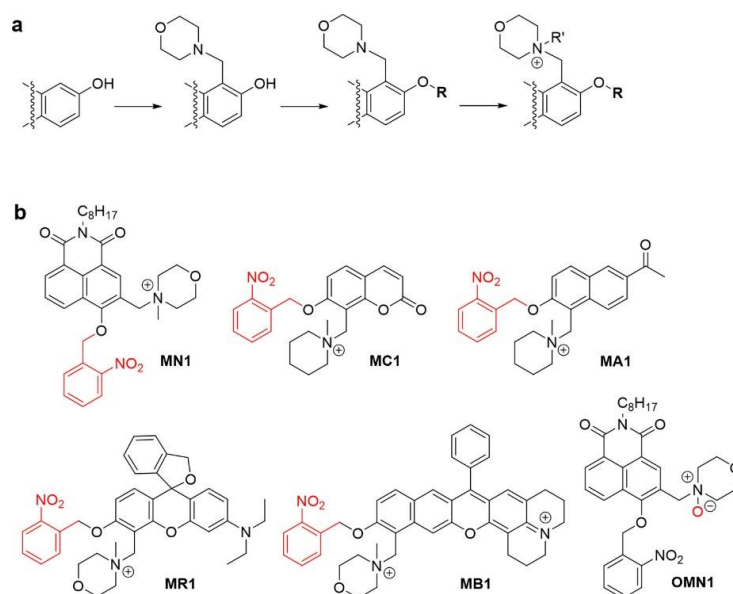
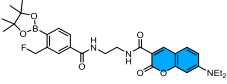
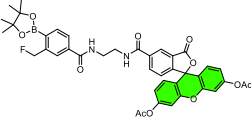
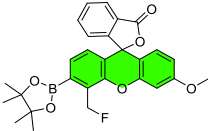
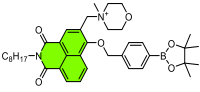


Figure 21. (a) Synthesis of the morpholinium derivatives. (b) The synthesized, *p*-nitrobenzyl caged probes. Reprinted with permission from [85], copyright 2022 American Chemical Society.

For a summary of ROS probes, see Table 11.

Table 11. ROS probes.

Structure ^a	ROS	Turn-On Ratio	λ (nm) abs/em ^b	Notes	Studied System	Ref.
	H ₂ O ₂ , ONOO ⁻	NA	360/470	in vitro model compound	in vitro	[83]
	H ₂ O ₂ , ONOO ⁻	ND	490/520	minor cellular toxicity, localized in vesicular organelles (phagosomes, endosomes, lysosomes, and autophagosomes)	in cellulo (Raw 264.7) ex-vivo (mouse brain tissue)	[83]
	H ₂ O ₂	25×	490/520	minor cellular toxicity, no specific localization	in cellulo (HeLA, A431, Raw 264.7, microglia-neuron cocultures)	[84]
	H ₂ O ₂ , ONOO ⁻ , ¹ O ₂ , O ₂ ⁻ , OH	30–70×	350/530	low cytotoxicity, highly localized in mitochondria and ER, can be used in two-photon microscopy	in cellulo (HeLA, Raw 264.7) ex-vivo (mouse kidney tissue)	[85]

^a fluorophores are colored according to the approximate emission maxima of the emissive form of the dye. ^b approximate absorption and emission maxima.

4. Conclusions

Herein we demonstrated the versatility of sensing and labeling with quinone methide function, focusing on enzyme activity and biologically relevant reactive oxygen species. The utilization of QM chemistry in biological media started with the development of mechanism-based/suicide inhibitors of enzymes. After enzyme-mediated removal of the substrate the generated electrophile QM can alkylate the active centrum, thus inactivating the enzyme. Activity-based probes also contain a recognition head tunable to the target function, and the activation is followed by covalent ligation as well. An attached reporter, either a fluorophore or an affinity-reporter, enables imaging or enrichment of the target motif, respectively. These probes frequently form covalent bonds outside the active site, although inactivating the enzyme is not without precedent. To control the effects displayed by the probe—i.e., whether it inactivates the enzyme or just labels it, or it labels proteins in the proximity of the enzyme—the fine-tuning of the applied leaving group is expedient. The most commonly used leaving group is fluoride, in the form of a monofluoromethyl or a difluoromethyl group. The former generates a more reactive QM but, in many cases, poses stability problems. The latter is stable, but the less reactive QM can diffuse further from the activation site. The third commonly used leaving group is the carbamate, which is stable and gives the same QM as the monofluoromethyl derivatives. Furthermore, the carbamate can have functional substituents, for example FRET acceptors (quenchers or fluorophores) that are removed upon activation. A wide range of fluorophores and fluorogenic dyes were applied, accomplishing sensitive, selective labeling, and retained spatial resolution with negligible background fluorescence, even under no-wash conditions and in live animals. This methodology is especially advantageous in live animals because the covalent ligation prevents rapid clearance of the dye.

We gave a detailed summary of protein labeling, focusing on chemical activation such as enzyme activity, but the application of QM chemistry goes beyond this. Photochemical methods to generate QMs and ways of application [86] were not outlined, although nonspecific protein labeling was accomplished with photoactivatable QMs as well [87–90]. The ability of DNA alkylating and cross-linking also widens the scope of biological applications [91–96]. Although the utility of QMs is obvious, there is still much room for

improvement in the future. There are already examples of small molecule enzymatic probes suitable for two-photon microscopy [97], and these can be modified with a latent QM for covalent labeling. In vivo deep tissue imaging could also benefit from the use of NIR-II dyes (λ : 1000–1700 nm) [98], and this requires development in the area of NIR-II dyes as well, as there are not yet many examples of NIR-II enzymatic probes [99]. The fluorophores in this review cover the whole visible spectrum, allowing for multi-color labeling that could help in visualizing multiple events. In view of the versatility and the increasing potential in quinone methide-based applications, they surely will help further deepen our understanding of complex phenomena in living systems.

Author Contributions: Writing—original draft preparation, D.K.; writing—review and editing, A.K. All authors have read and agreed to the published version of the manuscript.

Funding: This work has been implemented with the support provided by the Ministry of Innovation and Technology of Hungary from the National Research, Development and Innovation Fund, and financed under the NKFIH-FK-137589 funding scheme. This work was supported by the ÚNKP-22-3 New National Excellence Program of the Ministry for Innovation and Technology from the source of the National Research, Development and Innovation Fund (D.K.). A.K. is grateful for the support of the Hungarian Academy of Sciences (BO/00154/21/7 János Bolyai Research Scholarship).

Institutional Review Board Statement: Not applicable.

Informed Consent Statement: Not applicable.

Data Availability Statement: Not applicable.

Conflicts of Interest: The authors declare no conflict of interest.

References

1. Ravikumar, Y.; Nadarajan, S.P.; Yoo, T.H.; Lee, C.-S.; Yun, H. Unnatural amino acid mutagenesis-based enzyme engineering. *Trends Biotechnol.* **2015**, *33*, 462–470. [[CrossRef](#)] [[PubMed](#)]
2. Rawale, D.G.; Thakur, K.; Adusumalli, S.R.; Rai, V. Chemical Methods for Selective Labeling of Proteins. *Eur. J. Org. Chem.* **2019**, *2019*, 6749–6763. [[CrossRef](#)]
3. Scinto, S.L.; Bilodeau, D.A.; Hincapie, R.; Lee, W.; Nguyen, S.S.; Xu, M.; am Ende, C.W.; Finn, M.G.; Lang, K.; Lin, Q.; et al. Bioorthogonal chemistry. *Nat. Rev. Methods Prim.* **2021**, *1*, 30. [[CrossRef](#)] [[PubMed](#)]
4. Singh, J. The Ascension of Targeted Covalent Inhibitors. *J. Med. Chem.* **2022**, *65*, 5886–5901. [[CrossRef](#)] [[PubMed](#)]
5. Fang, Y.; Zou, P. Photocatalytic proximity labeling for profiling the subcellular organization of biomolecules. *ChemBioChem* **2023**. [[CrossRef](#)]
6. Fischer, N.H.; Oliveira, M.T.; Diness, F. Chemical modification of proteins—challenges and trends at the start of the 2020s. *Biomater. Sci.* **2023**. [[CrossRef](#)]
7. Turner, A.B. Quinone methides. *Q. Rev. Chem. Soc.* **1964**, *18*, 347–360. [[CrossRef](#)]
8. Toteva, M.M.; Richard, J.P. The Generation and Reactions of Quinone Methides. *Adv. Phys. Org. Chem.* **2011**, *45*, 39–91.
9. Goodman, J.L.; Peters, K.S.; Lahti, P.M.; Berson, J.A. Picosecond Absorption Studies on *m*-Naphthoquinomethane. Singlet-Triplet Intersystem Crossing. *J. Am. Chem. Soc.* **1985**, *107*, 276–277. [[CrossRef](#)]
10. Béchet, J.-J.; Dupaix, A.; Yon, J.; Wakselman, M.; Robert, J.-C.; Vilkas, M. Inactivation of α -Chymotrypsin by a Bifunctional Reagent, 3,4-Dihydro-3,4-dibromo-6-bromomethylcoumarin. *Eur. J. Biochem.* **1973**, *35*, 527–539. [[CrossRef](#)]
11. Wakselman, M. 1,4- and 1,6-Eliminations from Hydroxy- and Amino-Substituted Benzyl Systems: Chemical and Biochemical Applications. *Nouv. J. Chim.* **1983**, *7*, 439–447. [[CrossRef](#)]
12. Harper, J.W.; Powers, J.C. 3-Alkoxy-7-amino-4-chloroisocoumarins: A New Class of Suicide Substrates for Serine Proteases. *J. Am. Chem. Soc.* **1984**, *106*, 7619–7621. [[CrossRef](#)]
13. Halazy, S.; Danzin, C.; Ehrhard, A.; Gerhart, F. 1,1-Difluoroalkyl glucosides: A new class of enzyme-activated irreversible inhibitors of α -glucosidases. *J. Am. Chem. Soc.* **1989**, *111*, 3484–3485. [[CrossRef](#)]
14. Halazy, S.; Berges, V.; Ehrhard, A.; Danzin, C. *Ortho*- and *para*-(difluoromethyl)aryl- β -d-glucosidases. *Bioorg. Chem.* **1990**, *18*, 330–344. [[CrossRef](#)]
15. Wakselman, M.; Cerutti, I.; Chany, C. Nitrobenzyl esters as potential conjugated alkylating and differentiation promoting agents: Antitumor effect in vivo. *Eur. J. Med. Chem.* **1990**, *25*, 519–526. [[CrossRef](#)]
16. Wakselman, M.; Xie, J.; Mazaleyrat, J.-P. New Mechanism-Based Inactivators of Trypsin-like Proteinases. Selective Inactivation of Urokinase by Functionalized Cyclopeptides Incorporating a Sulfoniomethyl-Substituted *m*-Aminobenzoic Acid Residue. *J. Med. Chem.* **1993**, *36*, 1539–1547. [[CrossRef](#)]

17. Myers, J.K.; Widlanski, T.S. Mechanism-based inactivation of prostatic acid phosphatase. *Science* **1993**, *262*, 1451–1453. [[CrossRef](#)] [[PubMed](#)]
18. Wang, Q.; Dechert, U.; Jirik, F.; Withers, S.G. Suicide Inactivation of Human Prostatic Acid Phosphatase and a Phosphotyrosine Phosphatase. *Biochem. Biophys. Res. Commun.* **1994**, *200*, 577–583. [[CrossRef](#)]
19. Born, T.L.; Myers, J.K.; Widlanski, T.S.; Rusnak, F. 4-(Fluoromethyl)phenyl phosphate acts as a mechanism-based inhibitor of calcineurin. *J. Biol. Chem.* **1995**, *270*, 25651–25655. [[CrossRef](#)]
20. Myers, J.K.; Cohen, J.D.; Widlanski, T.S. Substituent Effects on the Mechanism-Based Inactivation of Prostatic Acid Phosphatase. *J. Am. Chem. Soc.* **1995**, *117*, 11049–11054. [[CrossRef](#)]
21. Massière, F.; Badet-Denisot, M.-A.; René, L.; Badet, B. Design, Synthesis and Evaluation of the First Mechanism-Based Inhibitor of Glucosamine 6-Phosphate Synthase. *J. Am. Chem. Soc.* **1997**, *119*, 5748–5749. [[CrossRef](#)]
22. Araújo, R.; Anhalt, E.; René, L.; Badet-Denisot, M.-A.; Courvalin, P.; Badet, B. Mechanism-Based Inactivation of VanX, a d-Alanyl-d-alanine Dipeptidase Necessary for Vancomycin Resistance. *Biochemistry* **2000**, *39*, 15971–15979. [[CrossRef](#)] [[PubMed](#)]
23. Yaouancq, L.; Anissimova, M.; Badet-Denisot, M.-A.; Badet, B. Design and Evaluation of Mechanism-Based Inhibitors of d-Alanyl-d-alanine Dipeptidase VanX. *Eur. J. Org. Chem.* **2002**, *2002*, 3573–3579. [[CrossRef](#)]
24. Janda, K.D.; Lo, L.-C.; Lo, C.-H.L.; Sim, M.-M.; Wang, R.; Wong, C.-H.; Lerner, R.A. Chemical Selection for Catalysis in Combinatorial Antibody Libraries. *Science* **1997**, *275*, 945–948. [[CrossRef](#)]
25. Betley, J.R.; Cesaro-Tadic, S.; Mekhalifa, A.; Rickard, J.H.; Denham, H.; Partridge, L.J.; Plückthun, A.; Blackburn, G.M. Direct Screening for Phosphatase Activity by Turnover-Based Capture of Protein Catalysts. *Angew. Chem. Int. Ed.* **2002**, *41*, 775–777. [[CrossRef](#)]
26. Cesaro-Tardic, S.; Lagos, D.; Honegger, A.; Rickard, J.H.; Partridge, L.J.; Blackburn, G.M.; Plückthun, A. Turnover-based in vitro selection and evolution of biocatalysts from a fully synthetic antibody library. *Nat. Biotechnol.* **2003**, *21*, 679–685. [[CrossRef](#)]
27. Lo, L.-C.; Lo, C.-H.L.; Janda, K.D. A Versatile Mechanism-Based Reaction Probe for the Direct Selection of Biocatalysts. *Bioorg. Med. Chem. Lett.* **1996**, *6*, 2117–2120. [[CrossRef](#)]
28. Lo, L.-C.; Chiang, Y.-L.; Kuo, C.-H.; Liao, H.-K.; Chen, Y.-J.; Lin, J.-J. Study of the preferred modification sites of the quinone methide intermediate resulting from the latent trapping device of the activity probes for hydrolases. *Biochem. Biophys. Res. Commun.* **2005**, *326*, 30–35. [[CrossRef](#)]
29. Lo, L.-C.; Wang, H.-Y.; Wang, Z.-J. Design and Synthesis of an Activity Probe for Protein Tyrosine Phosphatases. *J. Chin. Chem. Soc.* **1999**, *46*, 715–718. [[CrossRef](#)]
30. Lo, L.-C.; Pang, T.-L.; Kuo, C.-H.; Chiang, Y.-L.; Wang, H.-Y.; Lin, J.-J. Design and Synthesis of Class-Selective Activity Probes for Protein Tyrosine Phosphatases. *J. Proteome Res.* **2002**, *1*, 35–40. [[CrossRef](#)]
31. Zhu, Q.; Huang, X.; Chen, G.Y.J.; Yao, S.Q. Activity-based fluorescent probes that target phosphatases. *Tetrahedron Lett.* **2003**, *44*, 2669–2672. [[CrossRef](#)]
32. Shen, K.; Qi, L.; Ravula, M.; Klimaszewski, K. Synthesis and peptide incorporation of an unnatural amino acid containing activity-based probe for protein tyrosine phosphatases. *Bioorg. Med. Chem. Lett.* **2009**, *19*, 3264–3267. [[CrossRef](#)] [[PubMed](#)]
33. Shen, K.; Qi, L.; Ravula, M. Facile Incorporation of a Phosphatase Activity-Dependent Quinone Methide Generating Motif into Phosphotyrosine. *Synthesis* **2009**, *22*, 3765–3768. [[CrossRef](#)]
34. Kalesh, K.A.; Pheng, T.L.; Lu, K.; Gao, L.; Wang, J.; Yao, S.Q. Peptide-based activity-based probes (ABPs) for target-specific profiling of proteintyrosine phosphatases (PTPs). *Chem. Commun.* **2010**, *46*, 589–591. [[CrossRef](#)]
35. Huang, Y.-Y.; Kuo, C.-C.; Chu, C.-Y.; Huang, Y.-H.; Hu, Y.-L.; Lin, J.-J.; Lo, L.-C. Development of activity-based probes with tunable specificity for protein tyrosine phosphatase subfamilies. *Tetrahedron* **2010**, *66*, 4521–4529. [[CrossRef](#)]
36. Polaske, N.W.; Kelly, B.D.; Ashworth-Sharpe, J.; Bieniarz, C. Quinone Methide Signal Amplification: Covalent Reporter Labeling of Cancer Epitopes using Alkaline Phosphatase Substrates. *Bioconjug. Chem.* **2016**, *27*, 660–666. [[CrossRef](#)]
37. Song, H.; Li, Y.; Xue, C.; Xie, H. Highly Efficient Multiple-Labeling Probes for the Visualization of Enzyme Activities. *Eur. J. Chem.* **2019**, *25*, 13994–14002. [[CrossRef](#)]
38. Li, X.; Gao, X.; Shi, W.; Ma, H. Design Strategies for Water-Soluble Small Molecular Chromogenic and Fluorogenic Probes. *Chem. Rev.* **2014**, *114*, 590–659. [[CrossRef](#)]
39. Ge, J.; Li, L.; Yao, S.Q. A self-immobilizing and fluorogenic unnatural amino acid that mimics phosphotyrosine. *Chem. Commun.* **2011**, *47*, 10939–10941. [[CrossRef](#)]
40. Li, Y.; Song, H.; Xue, C.; Fang, Z.; Xiong, L.; Xie, H. A self-immobilizing near-infrared fluorogenic probe for sensitive imaging of extracellular enzyme activity in vivo. *Chem. Sci.* **2020**, *11*, 5889–5894. [[CrossRef](#)]
41. Chen, Y.; Xue, C.; Wang, J.; Xu, M.; Li, Y.; Ding, Y.; Song, H.; Xu, W.; Xie, H. High-contrast and real-time visualization of membrane proteins in live cells with malachite green-based fluorogenic probes. *Chin. Chem. Lett.* **2022**, *33*, 1637–1642. [[CrossRef](#)]
42. Ichikawa, M.; Ichikawa, Y. A Mechanism-Based Affinity-Labeling Agent for Possible Use in Isolating N-Acetylglucosaminidase. *Bioorg. Med. Chem. Lett.* **2001**, *11*, 1769–1773. [[CrossRef](#)]
43. Tsai, C.-S.; Li, Y.-K.; Lo, L.-C. Design and Synthesis of Activity Probes for Glycosidases. *Org. Lett.* **2002**, *4*, 3607–3610. [[CrossRef](#)]
44. Kuroguchi, M.; Nishimura, S.-I.; Chuan Lee, Y. Mechanism-based Fluorescent Labeling of β -Galactosidases. *J. Biol. Chem.* **2004**, *279*, 44704–44712. [[CrossRef](#)]
45. Shie, T.-H.; Chiang, Y.-L.; Lin, J.-J.; Li, Y.-K.; Lo, L.-C. Facile synthesis toward the construction of an activity probe library for glycosidases. *Carbohydr. Res.* **2006**, *341*, 443–456. [[CrossRef](#)]

46. Lo, L.-C.; Chu, C.-Y.; Pan, Y.-R.; Wan, C.-F.; Li, Y.-K.; Lin, J.-J. Rapid and selective isolation of β -xylosidase through an activity-based chemical approach. *Biotechnol. J.* **2006**, *1*, 197–202. [[CrossRef](#)]
47. Komatsu, T.; Kikuchi, K.; Takakusa, H.; Hanaoka, K.; Ueno, T.; Kamiya, M.; Urano, Y.; Nagano, T. Design and Synthesis of an Enzyme Activity-Based Labeling Molecule with Fluorescence Spectral Change. *J. Am. Chem. Soc.* **2006**, *128*, 15946–15947. [[CrossRef](#)]
48. Kalidasan, K.; Su, Y.; Wu, X.; Yao, S.Q.; Uttamchandani, M. Fluorescence-activated cell sorting and directed evolution of α -N-acetylgalactosaminidases using a quenched activity-based probe (qABP). *Chem. Commun.* **2013**, *49*, 7237–7239. [[CrossRef](#)]
49. Kwan, D.H.; Chen, H.-M.; Ratananikom, K.; Hancock, S.M.; Watanabe, Y.; Kongsaree, P.T.; Samuels, A.L.; Withers, S.G. Self-Immobilizing Fluorogenic Imaging Agents of Enzyme Activity. *Angew. Chem. Int. Ed.* **2011**, *50*, 300–303. [[CrossRef](#)]
50. Cheng, T.-C.; Roffler, S.R.; Tzou, S.-C.; Chuang, K.-H.; Su, Y.-C.; Chuang, C.-H.; Kao, C.-H.; Chen, C.-S.; Harn, I.-H.; Liu, K.-Y.; et al. An Activity-Based Near-Infrared Glucuronide Trapping Probe for Imaging β -Glucuronidase Expression in Deep Tissues. *J. Am. Chem. Soc.* **2012**, *134*, 3103–3110. [[CrossRef](#)]
51. Hsu, Y.-L.; Nandakumar, M.; Lai, H.-Y.; Chou, T.-C.; Chu, C.-Y.; Lin, C.-H.; Lo, L.-C. Development of Activity-Based Probes for Imaging Human α -L-Fucosidases in Cells. *J. Org. Chem.* **2015**, *80*, 8458–8463. [[CrossRef](#)] [[PubMed](#)]
52. Nandakumar, M.; Hsu, Y.-L.; Lin, J.C.-Y.; Lo, C.; Lo, L.-C. Detection of Human α -L-Fucosidases by a Quinone Methide-Generating Probe: Enhanced Activities in Response to *Helicobacter pylori* Infection. *ChemBioChem* **2015**, *16*, 1555–1559. [[CrossRef](#)] [[PubMed](#)]
53. Doura, T.; Kamiya, M.; Obata, F.; Yamaguchi, Y.; Hiyama, T.Y.; Matsuda, T.; Fukamizu, A.; Noda, M.; Miura, M.; Urano, Y. Detection of *LacZ*-Positive Cells in Living Tissue with Single-Cell Resolution. *Angew. Chem. Int. Ed.* **2016**, *55*, 9620–9624. [[CrossRef](#)]
54. Kamiya, M.; Asanuma, D.; Kuranaga, E.; Takeishi, A.; Sakabe, M.; Miura, M.; Nagano, T.; Urano, Y. β -Galactosidase Fluorescence Probe with Improved Cellular Accumulation Based on a Spirocyclized Rhodol Scaffold. *J. Am. Chem. Soc.* **2011**, *133*, 12960–12963. [[CrossRef](#)]
55. Ito, H.; Kawamata, Y.; Kamiya, M.; Tsuda-Sakurai, K.; Tanaka, S.; Ueno, T.; Komatsu, T.; Hanaoka, K.; Okabe, S.; Miura, M.; et al. Red-Shifted Fluorogenic Substrate for Detection of *lacZ*-Positive Cells in Living Tissue with Single-Cell Resolution. *Angew. Chem. Int. Ed.* **2018**, *57*, 15702–15706. [[CrossRef](#)]
56. Chiba, M.; Kamiya, M.; Tsuda-Sakurai, K.; Fujisawa, Y.; Kosakamoto, H.; Kojima, R.; Miura, M.; Urano, Y. Activatable Photosensitizer for Targeted Ablation of *lacZ*-Positive Cells with Single-Cell Resolution. *ACS Cent. Sci.* **2019**, *5*, 1676–1681. [[CrossRef](#)]
57. Ichikawa, Y.; Kamiya, M.; Obata, F.; Miura, M.; Terai, T.; Komatsu, T.; Ueno, T.; Hanaoka, K.; Nagano, T.; Urano, Y. Selective Ablation of β -Galactosidase-Expressing Cells with a Rationally Designed Activatable Photosensitizer. *Angew. Chem. Int. Ed.* **2014**, *53*, 6772–6775. [[CrossRef](#)]
58. Jiang, J.; Tan, Q.; Zhao, S.; Song, H.; Hu, L.; Xie, H. Late-stage difluoromethylation leading to a self-immobilizing fluorogenic probe for the visualization of enzyme activities in live cells. *Chem. Commun.* **2019**, *55*, 15000–15003. [[CrossRef](#)]
59. Noguchi, K.; Shimomura, T.; Ohuchi, Y.; Ishiyama, M.; Shiga, M.; Mori, T.; Katayama, Y.; Ueno, Y. β -Galactosidase-Catalyzed Fluorescent Reporter Labeling of Living Cells for Sensitive Detection of Cell Surface Antigens. *Bioconjug. Chem.* **2020**, *31*, 1740–1744. [[CrossRef](#)]
60. Hirata, M.; Kogame, T.; Adachi, S.; Haga, H. Galactosidase-catalyzed fluorescence amplification method (GAFAM): Sensitive fluorescent immunohistochemistry using novel fluorogenic β -galactosidase substrates and its application in multiplex immunostaining. *Histochem. Cell Biol.* **2022**, 1–14. [[CrossRef](#)]
61. Hyun, J.Y.; Park, S.-H.; Park, C.W.; Kim, H.B.; Cho, J.W.; Shin, I. Trifunctional Fluorogenic Probes for Fluorescence Imaging and Isolation of Glycosidases in Cells. *Org. Lett.* **2019**, *21*, 4439–4442. [[CrossRef](#)] [[PubMed](#)]
62. Whidbey, C.; Sadler, N.C.; Nair, R.N.; Volk, R.F.; DeLeon, A.J.; Bramer, L.M.; Fansler, S.J.; Hansen, J.R.; Shukla, A.K.; Jansson, J.K.; et al. A Probe-Enabled Approach for the Selective Isolation and Characterization of functionally Active Subpopulations in the Gut Microbiome. *J. Am. Chem. Soc.* **2019**, *141*, 42–47. [[CrossRef](#)]
63. Luijckx, Y.M.C.A.; Henselijn, A.; Bosman, G.P.; Cramer, D.A.T.; Giesbers, K.C.A.P.; van 't Veld, E.M.; Boons, G.-J.; Heck, A.J.R.; Reiding, K.R.; Strijbis, K.; et al. Detection of Bacterial α -L-Fucosidases with an Ortho-Quinone Methide-Based Probe and Mapping of the Probe-Protein Adducts. *Molecules* **2022**, *27*, 1615. [[CrossRef](#)]
64. Liu, J.; Ma, X.; Cui, C.; Chen, Z.; Wang, Y.; Deenik, P.R.; Cui, L. Noninvasive NIR Imaging of Senescence via In Situ Labeling. *J. Med. Chem.* **2021**, *64*, 17969–17978. [[CrossRef](#)] [[PubMed](#)]
65. Lu, C.-P.; Ren, C.-T.; Lai, Y.-N.; Wu, S.-H.; Wang, W.-M.; Chen, J.-Y.; Lo, L.-C. Design of a Mechanism-Based Probe for Neuraminidase To Capture Influenza Viruses. *Angew. Chem. Int. Ed.* **2005**, *44*, 6888–6892. [[CrossRef](#)]
66. Hinou, H.; Kuroguchi, M.; Shimizu, H.; Nishimura, S.-I. Characterization of *Vibrio cholerae* Neuraminidase by a Novel Mechanism-Based Fluorescent Labeling Reagent. *Biochemistry* **2005**, *44*, 11669–11675. [[CrossRef](#)]
67. Zhu, R.; Wang, S.; Xue, Z.; Han, J.; Han, S. Senescence-associated sialidase revealed by an activatable fluorescence-on labeling probe. *Chem. Commun.* **2018**, *54*, 11566–11569. [[CrossRef](#)]
68. Gao, Z.; Thompson, A.J.; Paulson, J.C.; Withers, S.G. Proximity Ligation-Based Fluorogenic Imaging Agents for Neuraminidases. *Angew. Chem. Int. Ed.* **2018**, *57*, 13538–13541. [[CrossRef](#)]
69. Li, Y.; Xue, C.; Fang, Z.; Xu, W.; Xie, H. In Vivo Visualization of γ -Glutamyl Transpeptidase Activity with an Activatable Self-Immobilizing Near-Infrared Probe. *Anal. Chem.* **2020**, *92*, 15017–15024. [[CrossRef](#)]

70. Obara, R.; Kamiya, M.; Tanaka, Y.; Abe, A.; Kojima, R.; Kawaguchi, T.; Sugawara, M.; Takahashi, A.; Noda, T.; Urano, Y. γ -Glutamyltranspeptidase (GGT)-Activatable Fluorescence Probe for Durable Tumor Imaging. *Angew. Chem. Int. Ed.* **2021**, *60*, 2125–2129. [[CrossRef](#)]
71. Lu, C.-P.; Ren, C.-T.; Wu, S.-H.; Chu, C.-Y.; Lo, L.-C. Development of an Activity-Based Probe for Steroid Sulfatases. *ChemBioChem* **2007**, *8*, 2187–2190. [[CrossRef](#)]
72. Lenger, J.; Schröder, M.; Ennemann, E.C.; Müller, B.; Wong, C.-H.; Noll, T.; Dierks, T.; Hanson, S.R.; Sewald, N. Evaluation of sulfatase-directed quinone methide traps for proteomics. *Bioorg. Med. Chem.* **2012**, *20*, 622–627. [[CrossRef](#)] [[PubMed](#)]
73. Tai, C.-H.; Lu, C.-P.; Wu, S.-H.; Lo, L.-C. Synthesis and evaluation of turn-on fluorescent probes for imaging steroid sulfatase activities in cells. *Chem. Commun.* **2014**, *50*, 6116–6119. [[CrossRef](#)]
74. Park, H.-J.; Rhee, H.-W.; Hong, J.-I. Activity-based fluorescent probes for monitoring sulfatase activity. *Bioorg. Med. Chem. Lett.* **2012**, *22*, 4939–4941. [[CrossRef](#)]
75. Shao, Q.; Zheng, Y.; Dong, X.; Tang, K.; Yan, X.; Xing, B. A Covalent Reporter of β -Lactamase Activity for Fluorescent Imaging and Rapid Screening of Antibiotic-Resistant Bacteria. *Chem. Eur. J.* **2013**, *19*, 10903–10910. [[CrossRef](#)]
76. Mao, W.; Xia, L.; Wang, Y.; Xie, H. A Self-Immobilizing and Fluorogenic Probe for β -Lactamase Detection. *Chem. Asian J.* **2016**, *11*, 3493–3497. [[CrossRef](#)]
77. Sellars, J.-D.; Landrum, M.; Congreve, A.; Dixon, D.P.; Mosely, J.A.; Beeby, A.; Edwards, R.; Steel, P.G. Fluorescence quenched quinone methide based activity probes—a cautionary tale. *Org. Biomol. Chem.* **2010**, *8*, 1610–1618. [[CrossRef](#)]
78. Shi, Y.; Zhu, R.; Xue, Z.; Han, J.; Han, S. An in cellulo-activated multicolor cell labeling approach used to image dying cell clearance. *Analyst* **2019**, *144*, 4687–4693. [[CrossRef](#)]
79. Wang, S.; Tan, W.; Lang, W.; Qian, H.; Guo, S.; Zhu, L.; Ge, J. Fluorogenic and Mitochondria-Localizable Probe Enables Selective Labeling and Imaging of Nitroreductase. *Anal. Chem.* **2022**, *94*, 7272–7277. [[CrossRef](#)]
80. Cao, S.; Wang, Y.; Peng, X. ROS-Inducible DNA Cross-Linking Agent as a New Anticancer Prodrug Building Block. *Chem. Eur. J.* **2012**, *18*, 3850–3854. [[CrossRef](#)]
81. Cao, S.; Wang, Y.; Peng, X. The Leaving Group Strongly Affects H₂O₂-Induced DNA Cross-Linking by Arylboronates. *J. Org. Chem.* **2014**, *79*, 501–508. [[CrossRef](#)] [[PubMed](#)]
82. Wang, Y.; Fan, H.; Balakrishnan, K.; Lin, Z.; Cao, S.; Chen, W.; Fan, Y.; Guthrie, Q.A.; Sun, H.; Teske, K.A.; et al. Hydrogen peroxide activated quinone methide precursors with enhanced DNA cross-linking capability and cytotoxicity towards cancer cells. *Eur. J. Med. Chem.* **2017**, *133*, 197–207. [[CrossRef](#)] [[PubMed](#)]
83. Zhu, H.; Tamura, T.; Fujisawa, A.; Nishikawa, Y.; Cheng, R.; Takato, M.; Hamachi, I. Imaging and Profiling of Proteins under Oxidative Conditions in Cells and Tissues by Hydrogen-Peroxide-Responsive Labeling. *J. Am. Chem. Soc.* **2020**, *142*, 15711–15721. [[CrossRef](#)]
84. Iwashita, H.; Castillo, E.; Messina, M.S.; Swanson, R.A.; Chang, C.J. A tandem activity-based sensing and labeling strategy enables imaging of transcellular hydrogen peroxide signaling. *Proc. Natl. Acad. Sci. USA* **2021**, *118*, e2018513118. [[CrossRef](#)]
85. Jung, Y.L.; Sarkar, S.; Ha, J.; Park, S.B.; Ahn, K.H. Fluorophore Labeling of Proteins: A Versatile Trigger–Release–Conjugation Platform Based on the Quinone Methide Chemistry. *Bioconjug. Chem.* **2022**, *33*, 1543–1551. [[CrossRef](#)]
86. Basarić, N.; Mlinarić-Majerski, K.; Kralj, M. Quinone Methides: Photochemical Generation and its Application in Biomedicine. *Curr. Org. Chem.* **2014**, *18*, 3–18. [[CrossRef](#)]
87. Zlatić, K.; Antol, I.; Uzelac, L.; Mikecin Dražić, A.-M.; Kralj, M.; Bohne, C.; Basarić, N. Labeling of Proteins by BODIPY-Quinone Methides Utilizing Anti-Kasha Photochemistry. *ACS. Appl. Mater. Interfaces* **2020**, *12*, 347–351. [[CrossRef](#)]
88. Zlatić, K.; Cindrić, M.; Antol, I.; Uzelac, L.; Mihaljević, B.; Kralj, M.; Basarić, N. Wavelength dependent photochemistry of BODIPY-phenols and their applications in the fluorescent labeling of proteins. *Org. Biomol. Chem.* **2021**, *19*, 4891–4903. [[CrossRef](#)]
89. Kashima, H.; Kamiya, M.; Obata, F.; Kojima, R.; Nakano, S.; Miura, M.; Urano, Y. Photoactivatable fluorophores for durable labelling of individual cells. *Chem. Commun.* **2021**, *57*, 5802–5805. [[CrossRef](#)]
90. Zlatić, K.; Bogomolec, M.; Cindrić, M.; Uzelac, L.; Basarić, N. Synthesis, photophysical properties, anti-Kasha photochemical reactivity and biological activity of vinyl- and alkynyl-BODIPY derivatives. *Tetrahedron* **2022**, *124*, 132995. [[CrossRef](#)]
91. Wang, P.; Song, Y.; Zhang, L.; He, H.; Zhou, X. Quinone Methide Derivatives: Important Intermediates to DNA Alkylating and DNA Cross-linking Actions. *Curr. Med. Chem.* **2005**, *12*, 2893–2913. [[CrossRef](#)] [[PubMed](#)]
92. Percivalle, C.; Doria, F.; Freccero, M. Quinone Methides as DNA Alkylating Agents: An Overview on Efficient Activation Protocols for Enhanced Target Selectivity. *Curr. Org. Chem.* **2014**, *18*, 19–43. [[CrossRef](#)]
93. Huang, C.; Rokita, S.E. DNA alkylation promoted by an electron-rich quinone methide intermediate. *Front. Chem. Sci. Eng.* **2016**, *10*, 213–221. [[CrossRef](#)]
94. Hutchinson, M.A.; Deeyaa, B.D.; Byrne, S.R.; Williams, S.J.; Rokita, S.E. Directing Quinone Methide-Dependent Alkylation and Cross-Linking of Nucleic Acids with Quaternary Amines. *Bioconjug. Chem.* **2020**, *31*, 1486–1496. [[CrossRef](#)]
95. Deeyaa, B.D.; Rokita, S.E. Migratory ability of quinone methide-generating acridine conjugates in DNA. *Org. Biomol. Chem.* **2020**, *18*, 1671–1678. [[CrossRef](#)]
96. Byrne, S.R.; Rokita, S.E. Unraveling Reversible DNA Cross-Links with a Biological Machine. *Chem. Res. Toxicol.* **2020**, *33*, 2903–2913. [[CrossRef](#)]
97. Qian, L.; Li, L.; Yao, S.Q. Two-Photon Small Molecule Enzymatic Probes. *Acc. Chem. Res.* **2016**, *49*, 626–634. [[CrossRef](#)]

98. Wang, S.; Li, B.; Zhang, F. Molecular Fluorophores for Deep-Tissue Bioimaging. *ACS Cent. Sci.* **2020**, *6*, 1302–1316. [[CrossRef](#)]
99. Zhang, X.; Li, S.; Ma, H.; Wang, H.; Zhang, R.; Zhang, X.-D. Activatable NIR-II organic fluorescent probes for bioimaging. *Theranostics* **2022**, *12*, 3345–3371. [[CrossRef](#)]

Disclaimer/Publisher's Note: The statements, opinions and data contained in all publications are solely those of the individual author(s) and contributor(s) and not of MDPI and/or the editor(s). MDPI and/or the editor(s) disclaim responsibility for any injury to people or property resulting from any ideas, methods, instructions or products referred to in the content.